Atmospheric neutrino results from Super-Kamiokande

C. Bronner
Aug. 13th, 2018

Outline

- Atmospheric neutrinos to address open questions in neutrino oscillations
- Super-Kamiokande experiment
- Oscillation analysis
- Results
  - atmospheric neutrinos only
  - using external constraints
- Search for ν_τ appearance
- Future improvements

Neutrino oscillation
Open questions

Mass hierarchy:
$m_3 > m_2, m_1$?

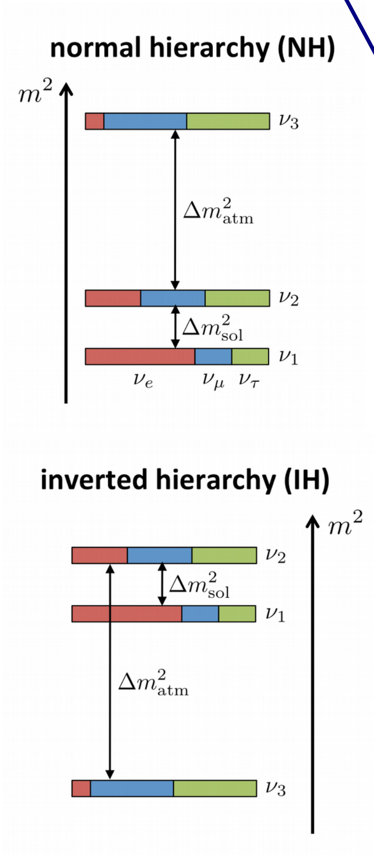

PDG 2017 summary table

Parameter	best-fit	3σ
Δm^2_{21} $[10^{-5}$ eV $^2]$	7.37	6.93 – 7.96
$\Delta m^2_{31(23)}$ $[10^{-3}$ eV $^2]$	2.56 (2.54)	2.45 – 2.69 (2.42 – 2.66)
$\sin^2\theta_{12}$	0.297	0.250 – 0.354
$\sin^2\theta_{23}$, $\Delta m^2_{31(32)} > 0$	0.425	0.381 – 0.615
$\sin^2\theta_{23}$, $\Delta m^2_{32(31)} < 0$	0.589	0.384 – 0.636
$\sin^2\theta_{13}$, $\Delta m^2_{31(32)} > 0$	0.0215	0.0190 – 0.0240
$\sin^2\theta_{13}$, $\Delta m^2_{32(31)} < 0$	0.0216	0.0190 – 0.0242
δ/π	1.38 (1.31)	2σ: (1.0 - 1.9) (2σ: (0.92-1.88))

Octant of θ_{23}:
$\theta_{23} > \pi/4$?
$\theta_{23} < \pi/4$?

Violation of CP symmetry in neutrino oscillations?

Degeneracies between those 3 questions

Atmospheric neutrinos
Interest for oscillation measurements

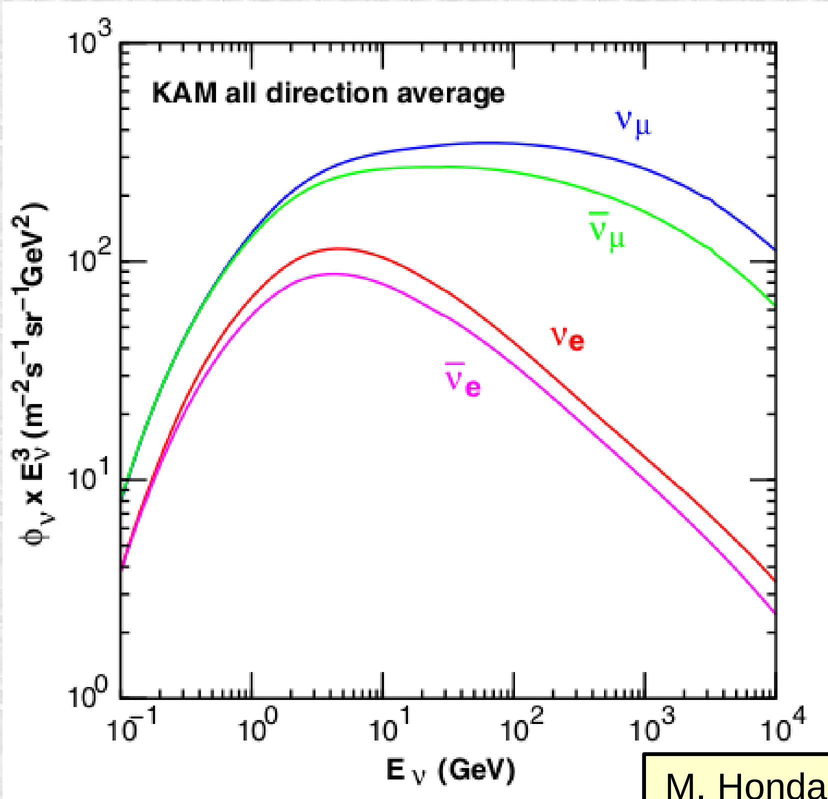

M. Honda

ν_μ, $\bar{\nu}_\mu$, ν_e, $\bar{\nu}_e$ over 5 decades in energy

L from 10 to 13000km

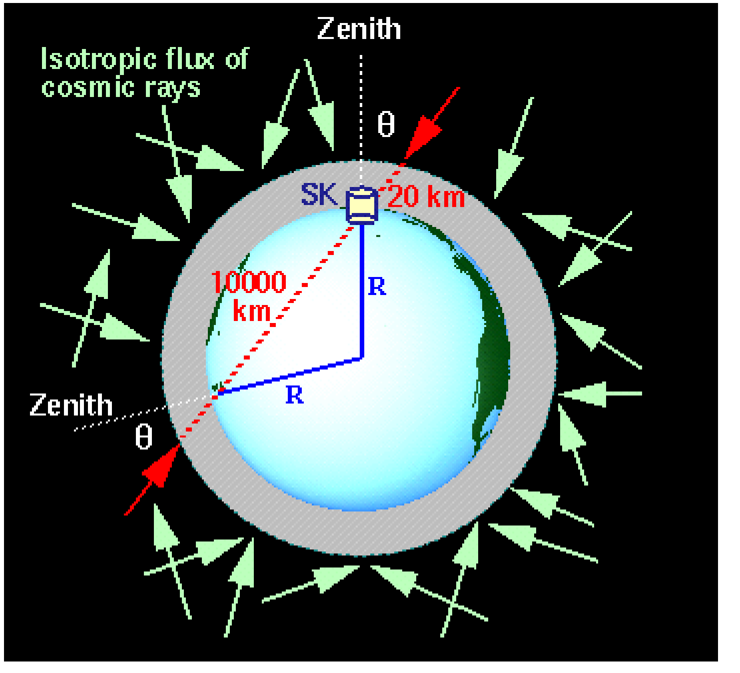

- Large range of neutrino energies and propagation lengths
- Oscillations dominated by $\nu_\mu \rightarrow \nu_\tau$
- Large statistics allow to study sub-dominant effects

Atmospheric neutrinos
Interest for oscillation measurements

Ability to study the open questions comes mainly from appearance channels $\nu_\mu \rightarrow \nu_e$ and $\bar{\nu}_\mu \rightarrow \bar{\nu}_e$

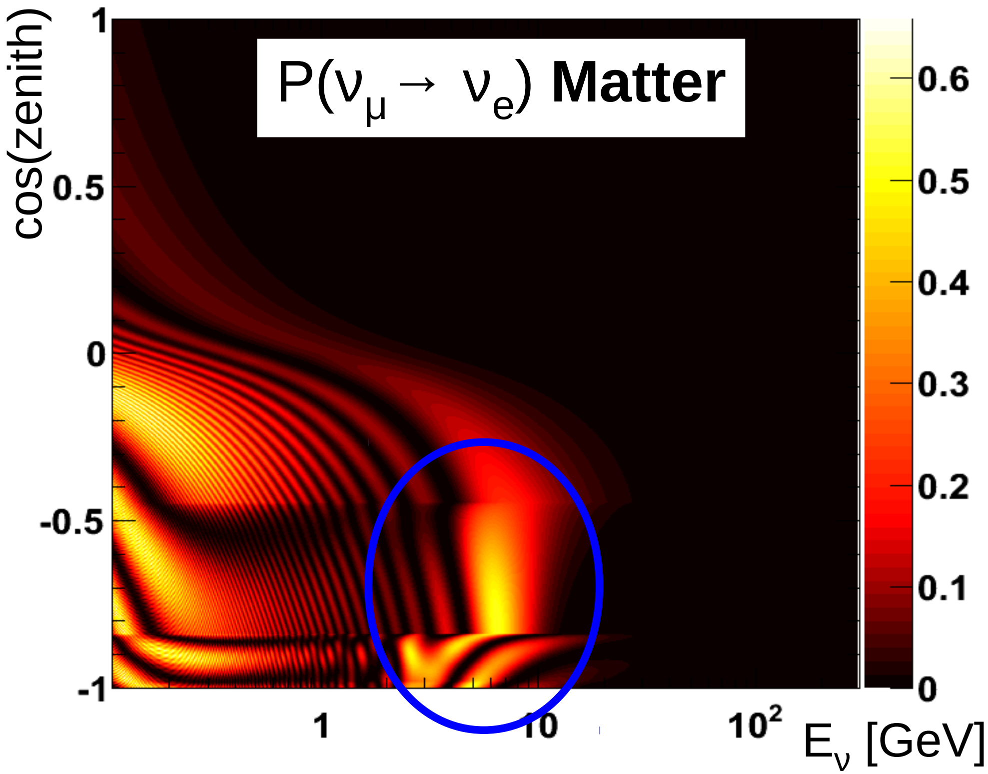

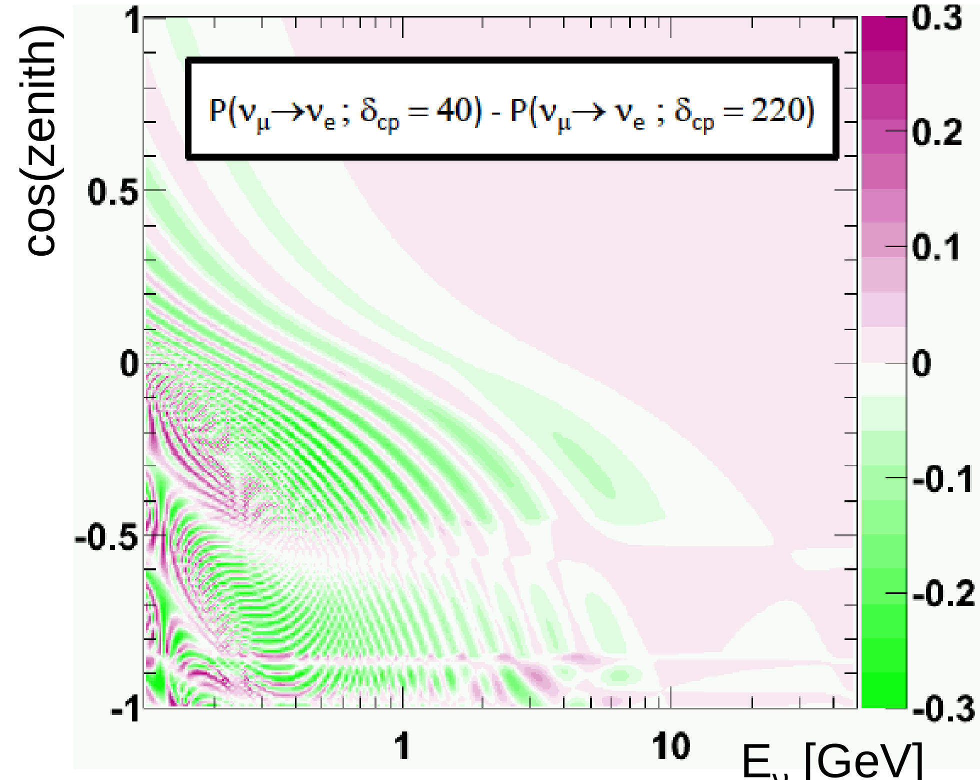

Resonance from matter effects

- Only for ν in NH and $\bar{\nu}$ in IH
  → **sensitive to the mass hierarchy**
- Size of the effect depends on $\sin^2(\theta_{23})$
  → **sensitive to θ_{23} octant**

δ_{CP} modifies the oscillation patterns

- Sensitivity from number of sub-GeV ν_e events
- More ν_e appearance events for δ~220-240º, and less for δ~40-45º

Super-Kamiokande experiment

- 50 kt (22.5 kt fiducial) water Cherenkov detector
- 1000m overburden
- Operational since 1996

Wide physics program:
- **Atmospheric neutrinos**
- Solar neutrinos
- Supernova neutrinos
- Proton decay
- Dark matter indirect detection

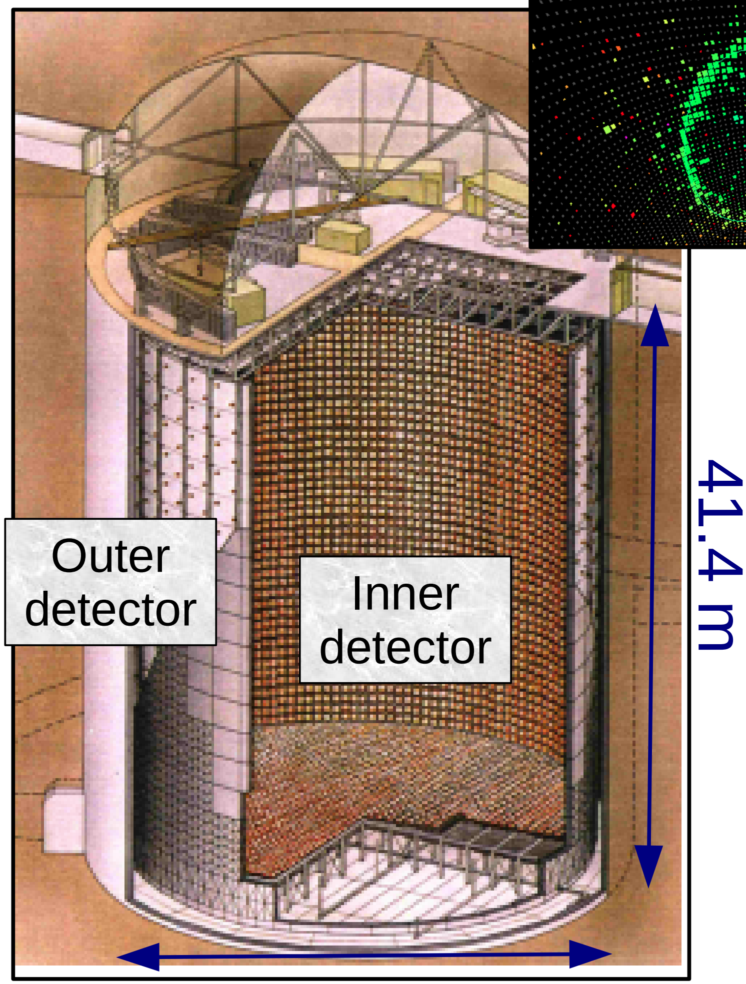

39.3 m

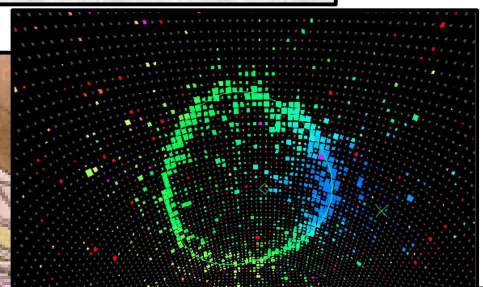

- Good separation between $\mu^\pm$ and $e^\pm$ (**separate ν_μ and ν_e CC interactions**)
  → Less than 1% mis-PID at 1 GeV
- No magnetic field: **cannot separate ν and $\bar{\nu}$ on an event by event basis**
- **Only detects charged particles above Cerenkov threshold and photons**
  → limitation for energy and directional reconstruction

Dataset

- 4 SK periods with different detector conditions over 20 years
- Total livetime: 5326 days (328 kton-year)
- 27505 muon-like and 20949 electron-like events

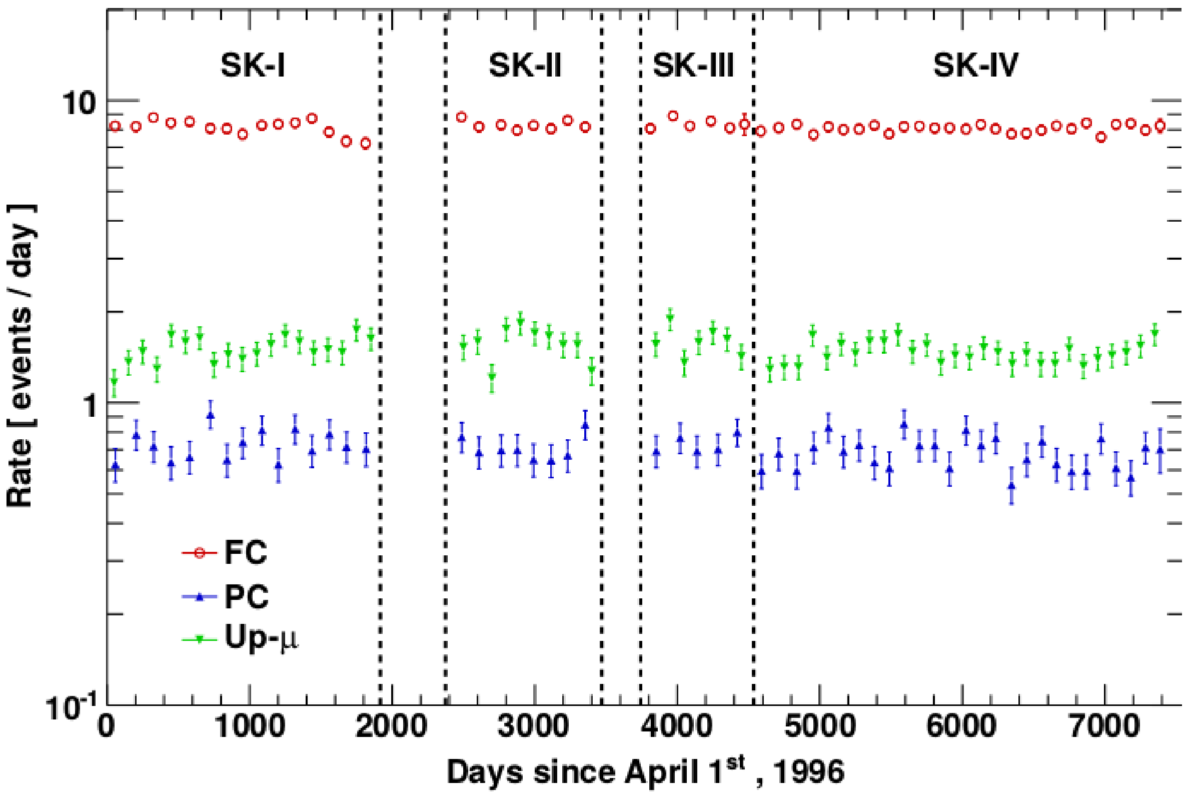

Stable event rates for the different topologies

Energy scale stability (stopping muon)

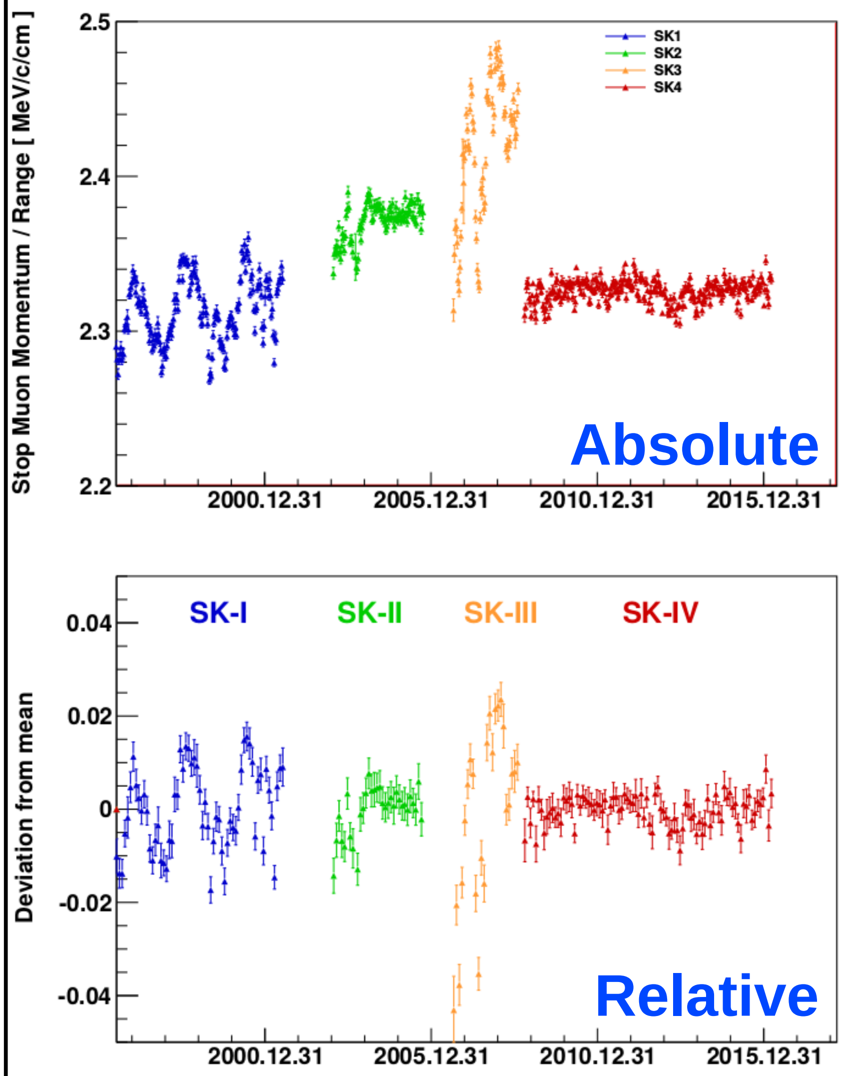

Oscillation analysis

- Maximum likelihood method
- Minimize χ^2 with respect to systematics for a grid of values of parameters to fit
- Minimization uses iterative matrix inversion method
- Binned χ^2 assuming Poisson statistics in each bin

Oscillation parameters

- $\sin^2(\theta_{13})$= 0.0219 ± 0.0012 (reactor)
- $\sin^2(\theta_{12})$= 0.304 ± 0.014 (solar+Kamland)
- Δm^2_{21}=(7.53 ± 0.18) × 10^{-5} eV^2/c^4 (solar+Kamland)
- $\sin^2(\theta_{23})$, $\Delta m^2_{32/31}$ and δ free

$$\chi^2 = 2\sum_n \left(E_n - \mathcal{O}_n + \mathcal{O}_n \ln \frac{\mathcal{O}_n}{E_n} \right) + \sum_i \left(\frac{\epsilon_i}{\sigma_i} \right)^2$$

Expected nb evts in bin n (E_n)

Observed nb of evts in bin n ($\mathcal{O}_n$)

Pull for syst. i (ϵ_i)

$$E_n = \sum_j E_{n,j} \left(1 + \sum_i f^i_{n,j} \epsilon_i \right)$$

Effect of a 1σ variation of syst. i on nb of evts in bin n for SK period j ($f^i_{n,j}$)

Predictions calculated separately for each SK period

- different detector configurations, water quality and performance → different MC simulations
- Some systematic uncertainties depend of the SK period
- Expectation from each period summed to compute χ^2

Atmospheric neutrino results

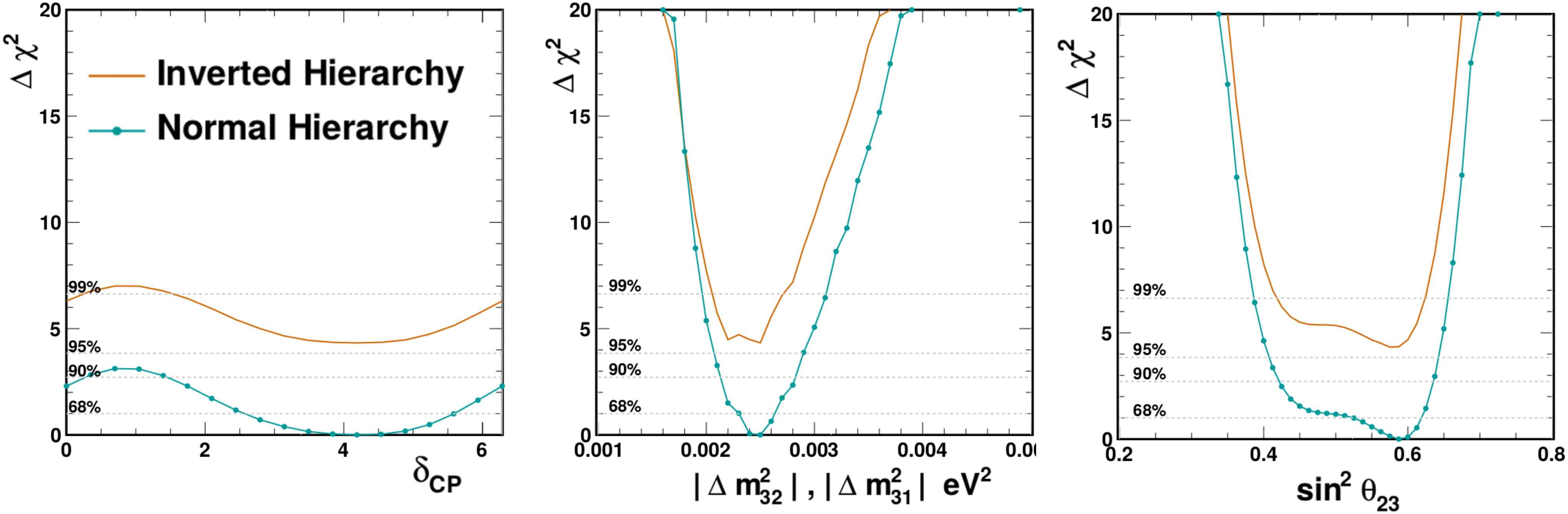

	χ^2	$\lvert\Delta m^2_{32/31}\rvert$	$\sin^2(\theta_{23})$	δ_{CP}
Normal hierarchy	571.33	2.5×10^{-3}	0.5875	4.18
Inverted hierarchy	575.66	2.5×10^{-3}	0.575	4.18

- **χ^2(NH)-χ^2(IH)=-4.33**
- P-value for this $\Delta\chi^2$ (true values of the parameters corresponding to the NH best fit point) is 0.027 for true IH
  → **Preference for the normal hierarchy hypothesis**

Analysis with external constraints

Motivations

- Uncertainty on value of $\sin^2(\theta_{23})$
  → uncertainty for MH determination
- Precise measurements of $\sin^2(\theta_{23})$ and $|\Delta m^2_{32}|$ by LBL experiments
- Both experiments have sensitivity to δ
- Combination can also break degeneracies in certain cases

Tokai To Kamioka (T2K)

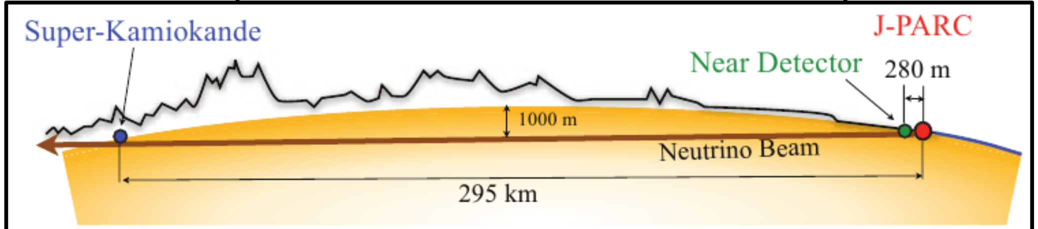

- Almost pure $\nu_\mu/\bar{\nu}_\mu$ beam
- L=295 km from J-PARC to Super-K
- Near detector complex to constrain systematic uncertainties

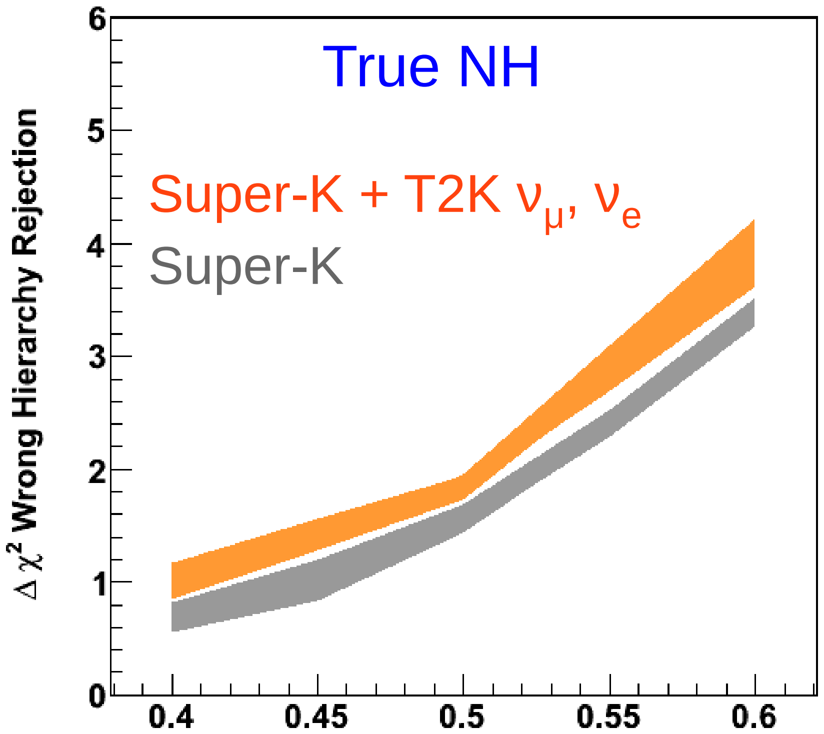

Error bands: uncertainty due to unknown δ value

- **NOT** a joint analysis between the 2 collaborations.
- Use SK tools to build a model of T2K and fit data based on publicly available information
- Uses T2K data and analysis from PRD 91, 072010 (2015) – not latest results (6.57e20 POT in ν-mode, no $\bar{\nu}$-mode data, no appearance CC1π sample, not using new reconstruction and fiducial volume)

Results with external constraints

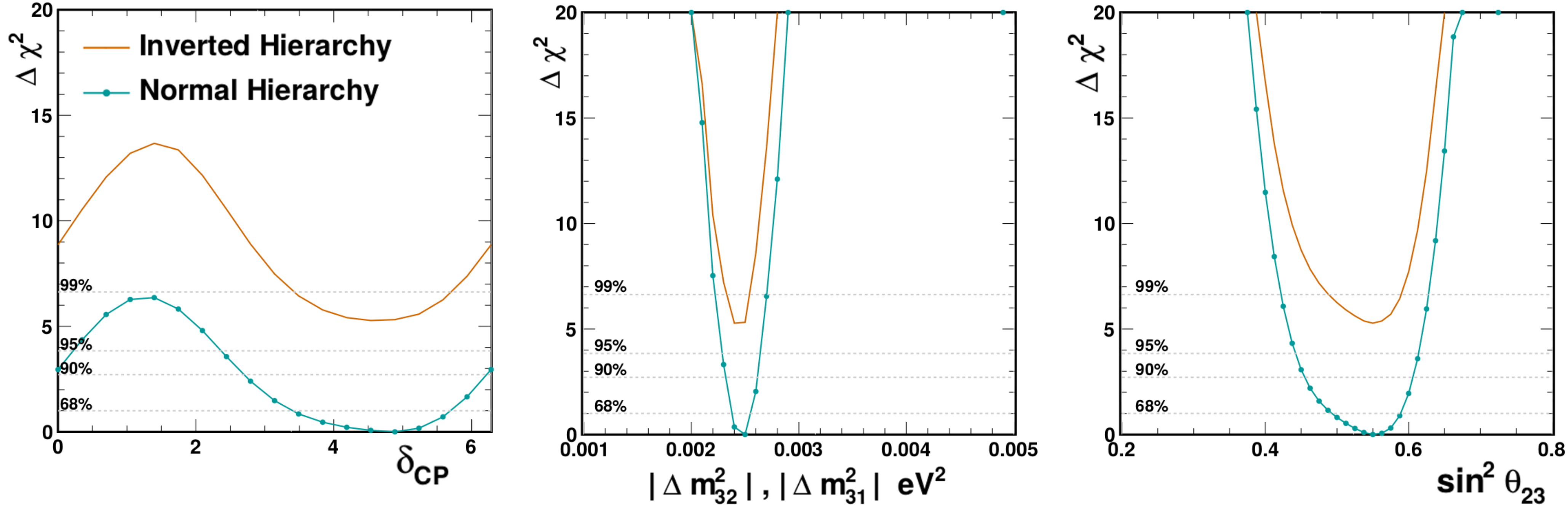

	χ^2	$\lvert\Delta m^2_{32/31}\rvert$	$\sin^2(\theta_{23})$	δ_{CP}
Normal hierarchy	639.43	2.50×10^{-3}	0.550	4.88
Inverted hierarchy	644.70	2.40×10^{-3}	0.550	4.54

- **χ^2(NH)-χ^2(IH)=-5.27**
- P-value for this $\Delta\chi^2$ (true values of the parameters corresponding to the NH best fit point) is 0.023 for true IH
  → **Slightly stronger preference for the normal hierarchy**

Mass hierarchy Significance

- MH significance does not go as √(χ2)
  → compute p-values using toy MC
- Limited sensitivity at current statistics
  → Also compute CLs values
- Significance depend on true values of θ_{23} and δ
  → Compute for different true values

Plot for SK atmospheric only

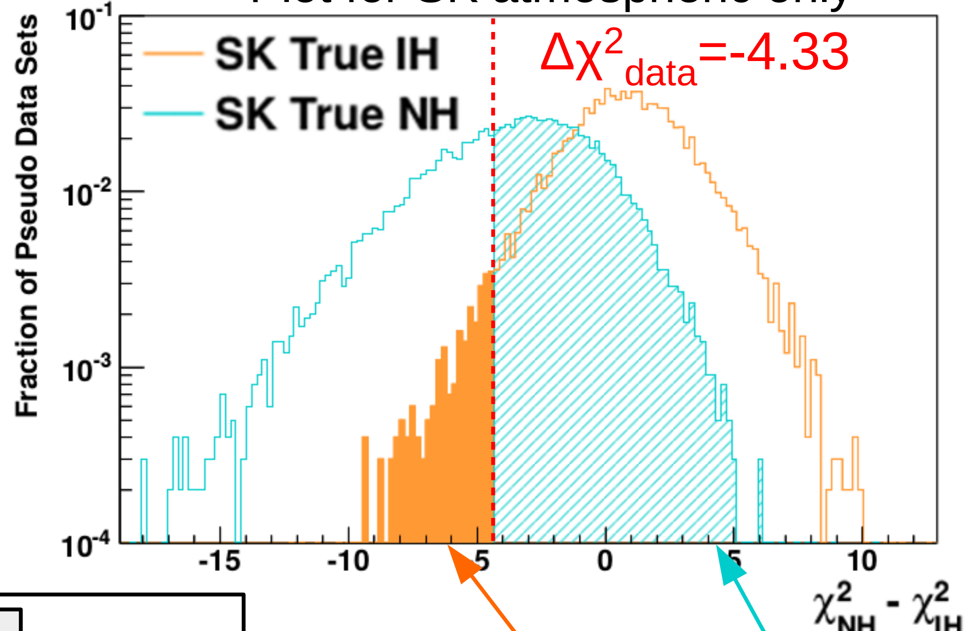

P-values and CLs for IH exclusion

P-values	Lower	Best fit	Upper
SK only	0.012	0.027	0.020
SK+T2K model	0.004	0.023	0.024

CLs	Lower	Best fit	Upper
SK only	0.181	0.070	0.033
SK+T2K model	0.081	0.075	0.056

$$CL_s = \frac{p_0(IH)}{1 - p_0(NH)}$$

Lower/upper edges of the 90% CL intervals for $\sin^2(\theta_{23})$ and δ

Atmospheric parameters

90% CL contours for the normal hierarchy case

- Super-K atmospheric only measurement compatible with other experiments results
- In the analysis using T2K model, result dominated by T2K data

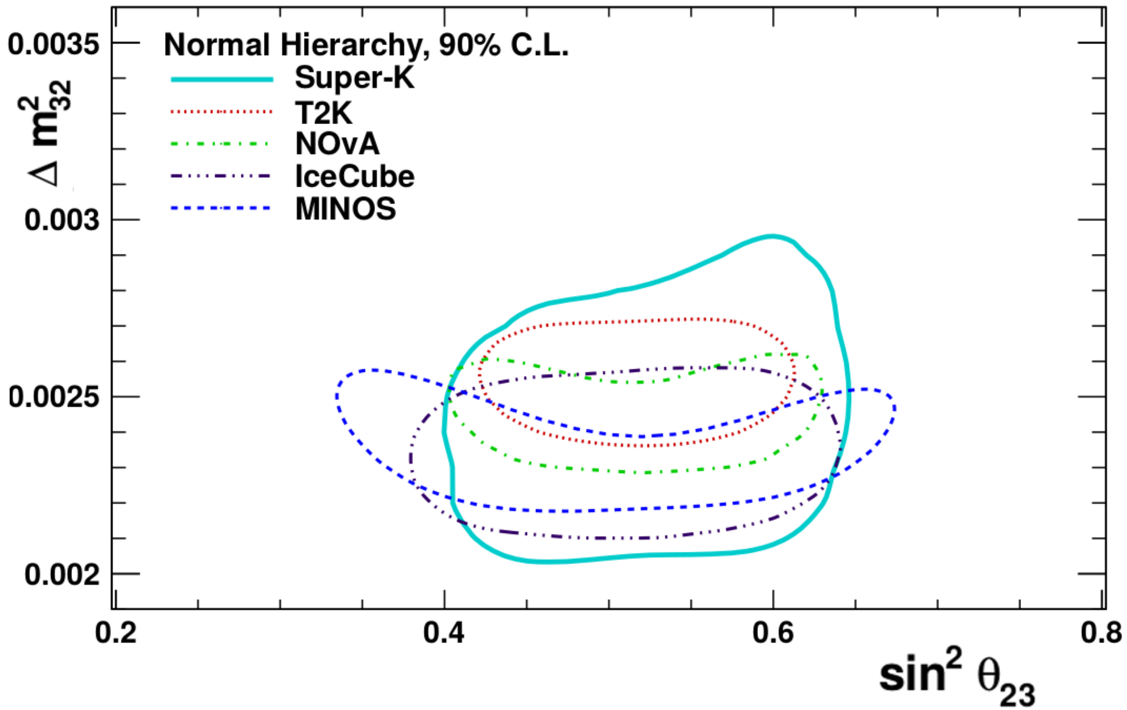

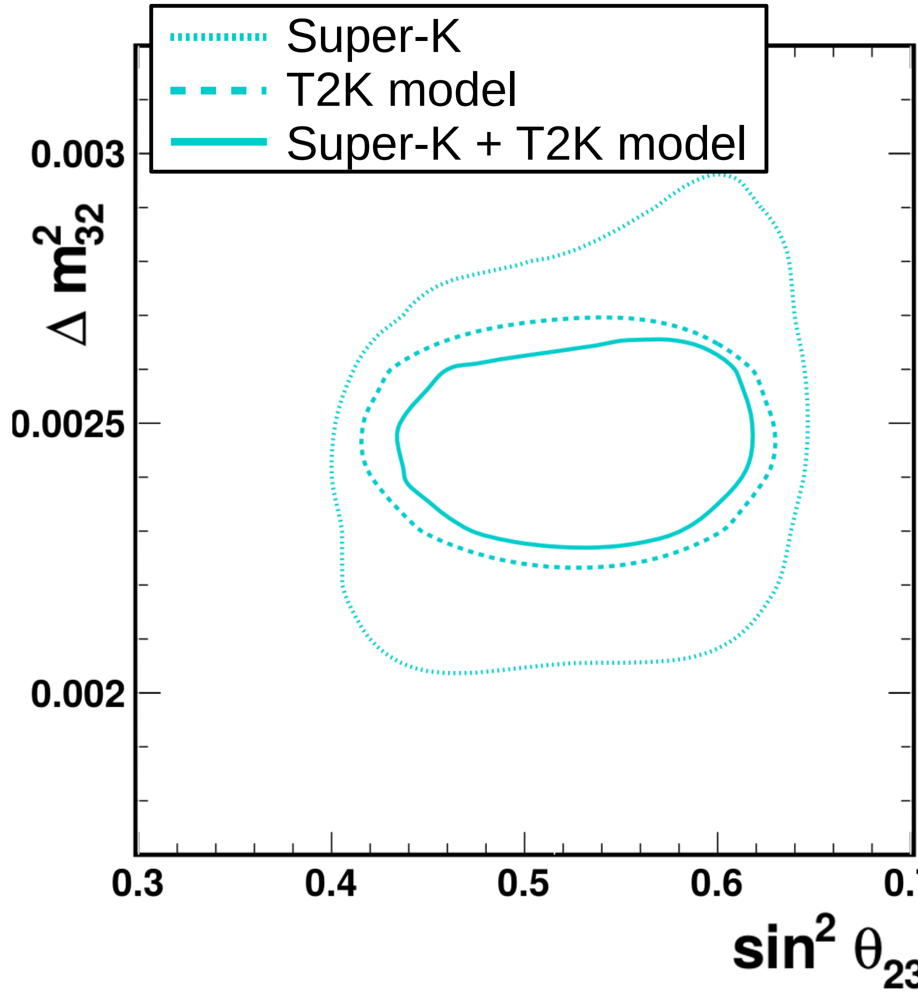

Notes:

- T2K contours for comparisons from PRL. 118, 151801 (2017), while model uses PRD 91, 072010 (2015)
- NOvA contours as presented in Jan. 2018 Fermilab JTEP seminar

ν_τ appearance

- No primary ν_τ atmospheric flux, but appear from oscillations
- Expect to detect ~1 ν_τ/year/kton in Super-K
- Only upward going (need L>4100 km)
  → down going sample can be used as a control sample for background

CC ν_τ threshold ~3.5 GeV

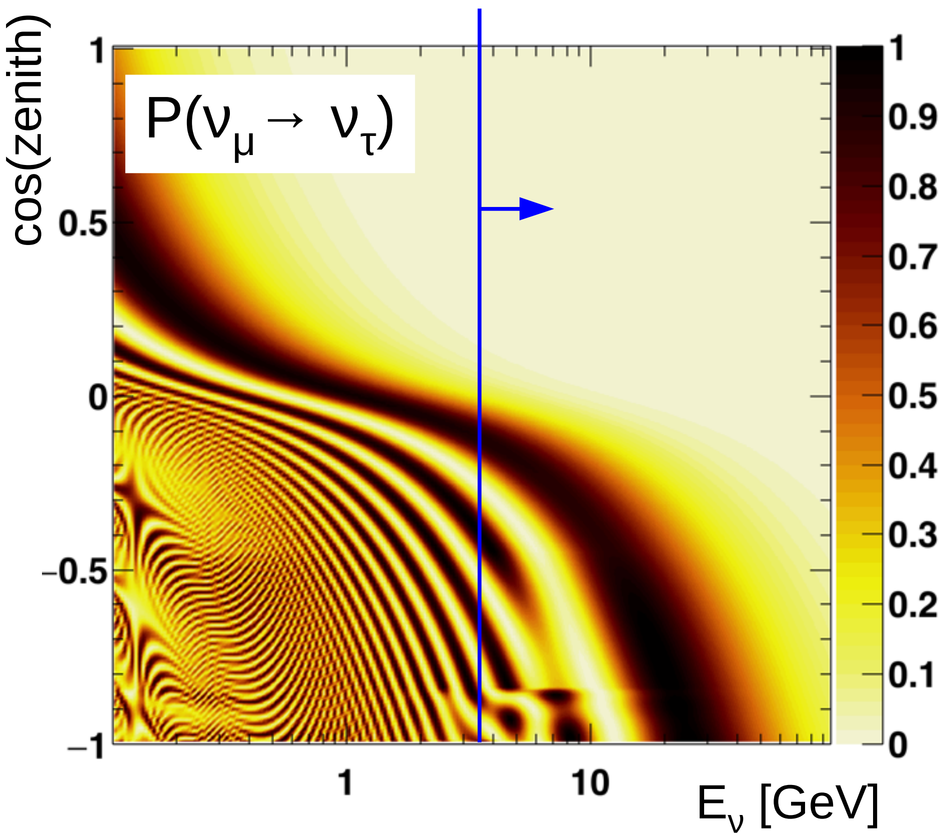

Can use NN to separate CC ν_τ events (τ hadronic decay) from ν_e/ν_μ bkg

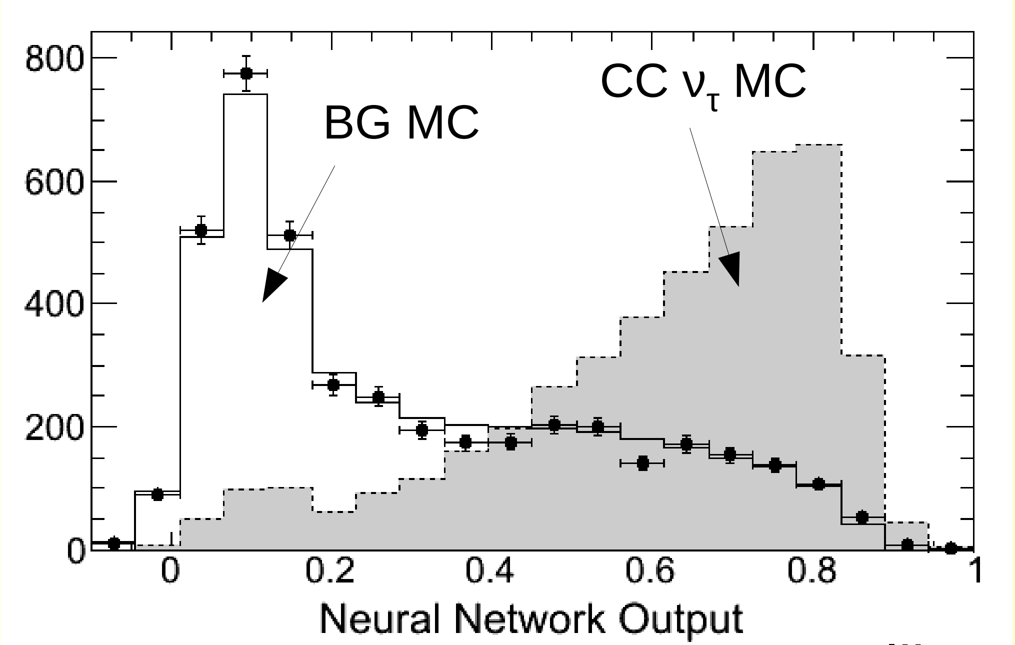

BG-like ⟷ τ-like

ν_τ appearance Results

- Unbinned maximal likelihood fit of 2D PDF
- Fit for CC ν_τ normalization "α"

Data = **α** x Signal + Background + syst.

$$\sum_i \epsilon_i \left(PDF_i^{BG} + PDF_i^{sig} \right)$$

Variation of syst i in σ (has gaussian constraint)

Effect of 1σ variation of syst i on 2D PDF

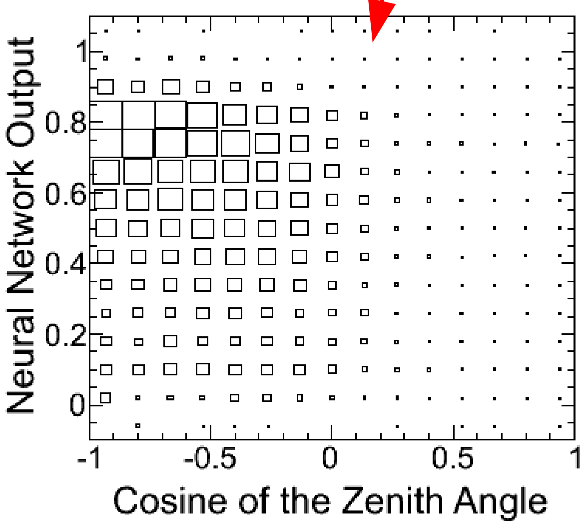

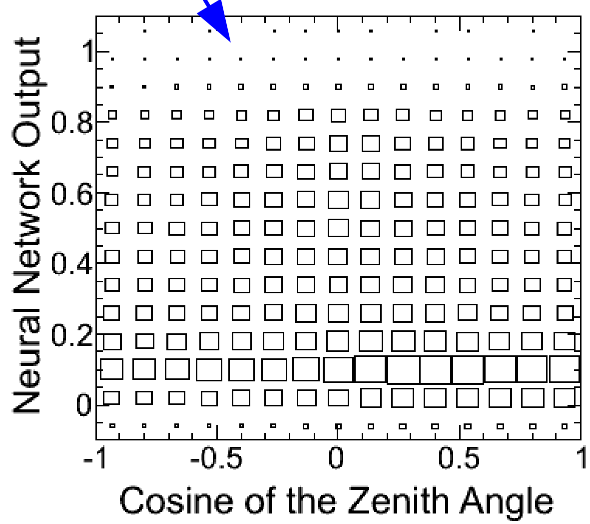

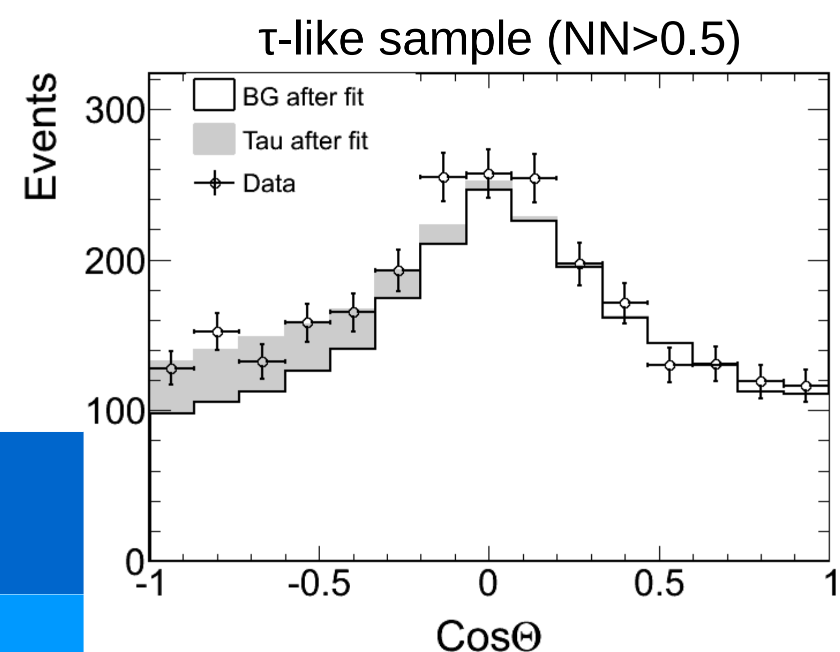

Mass Hierarchy	α	Significance
Normal	1.47 ± 0.32	4.6σ
Inverted	1.57 ± 0.31	5.0σ

arXiv:1711.09436 [hep-ex]

ν_τ appearance
Cross-section measurement

- Can use this dataset to measure ν_τ cross-section
- Scale theoretical (MC) cross section by α from ν_τ appearance fit
- Cannot separate ν_τ and $\bar{\nu}_\tau$ → flux average of ν_τ and $\bar{\nu}_\tau$ cross-sections

$$< \sigma_{measured} > = \boldsymbol{\alpha} \times < \sigma_{theory} >$$

$< \sigma_{theory} > = 0.64 \times 10^{-38}\ cm^2$

$\alpha = 1.47 \pm 0.32$

$$\mathbf{< \sigma_{measured} > = (0.94 \pm 0.20) \times 10^{-38}\ cm^2}$$

Agrees with theory within 1.5σ

(Flux average on 3.5-70 GeV)

$< \sigma_{theory} >$ = MC flux x dσ/dE

dσ/dE from NEUT generator

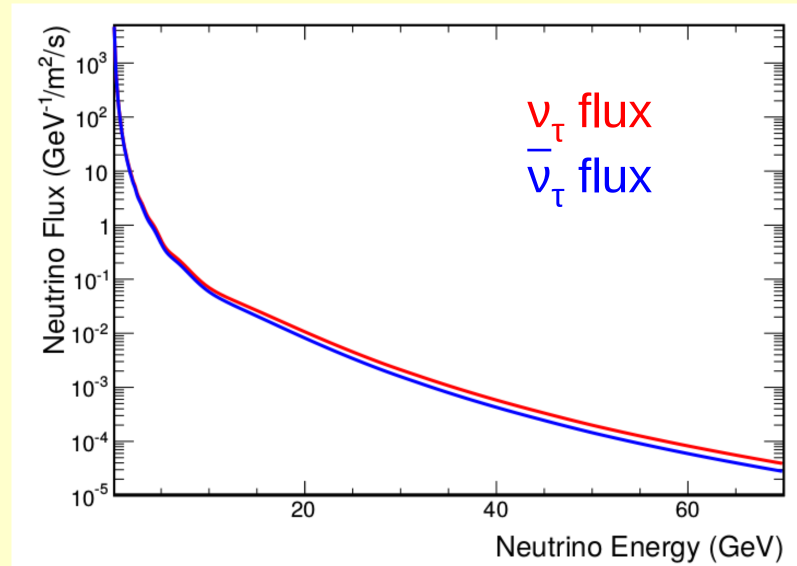

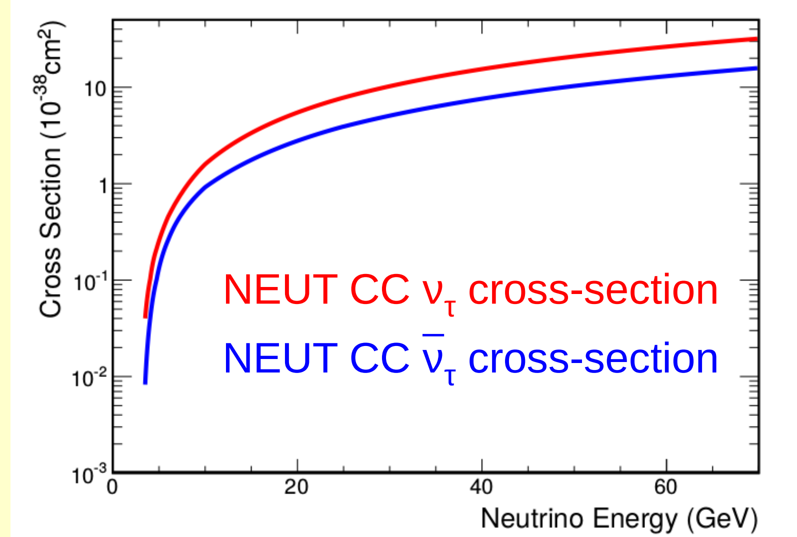

Future improvements
Use tau NN for oscillation analysis

- Up/down asymmetric group of events with normalization uncertainties are major backgrounds for mass hierarchy
- CC ν_τ cross-section has 25% uncertainty
- Can use NN output variable as an additional PDF variable for samples sensitive to the mass hierarchy

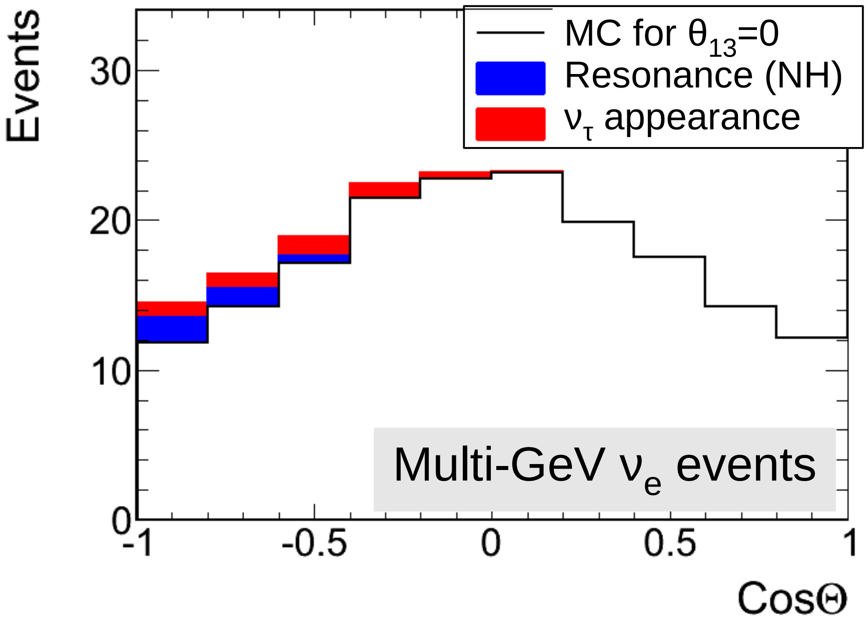

NN ouput can be used to isolate ν_τ events (example: cut at NN=0.5)

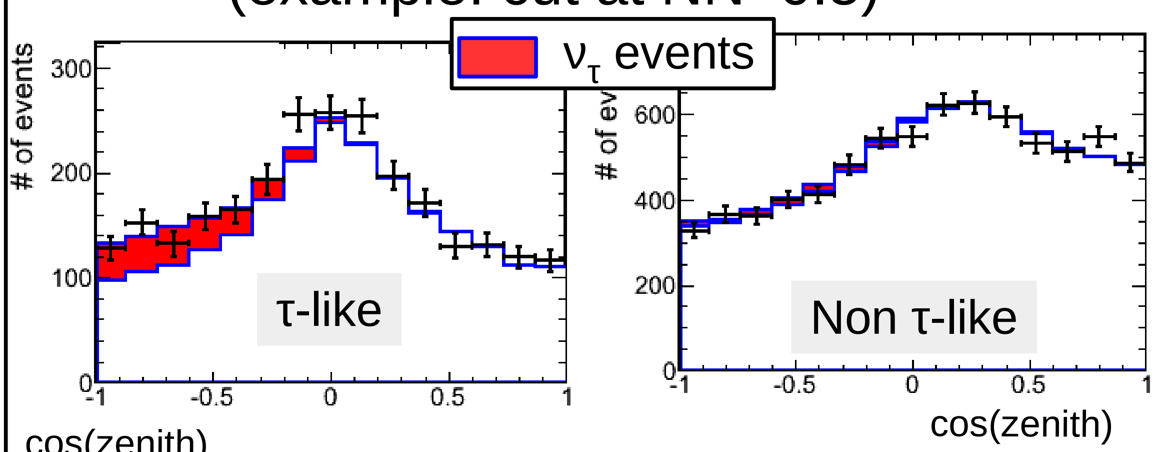

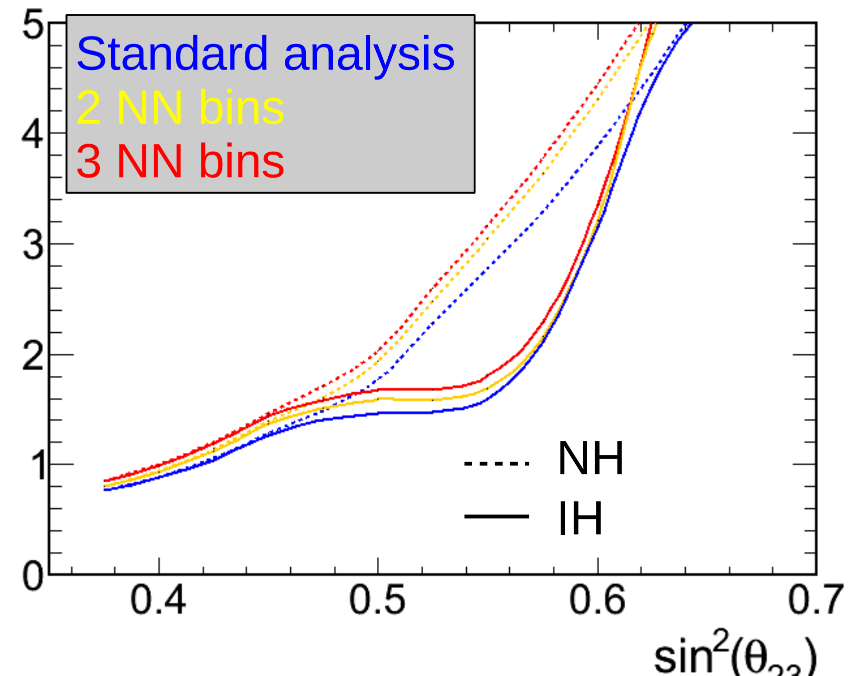

Future improvements
New event reconstruction algorithm

- Maximum likelihood method using charge and time information from each PMT
- Improved PID performance, as well as vertex and momentum resolution
- Already used in T2K

Improved performance allows to consider larger fiducial volume

Dist(vertex, wall)>2m
(FV=~70% ID volume)

↓ ?

Dist(vertex, wall)>0.5m
(FV=~83% ID volume)

Momentum resolution, SR e-like events

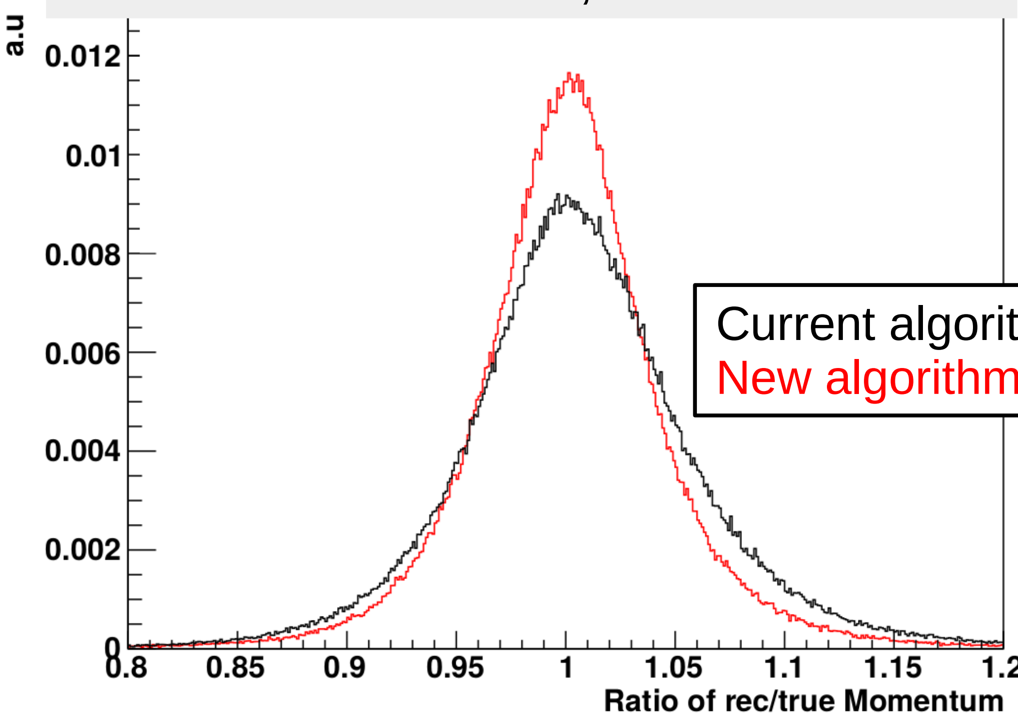

Probability to mis-identify a $\mu^{\pm}$ as an $e^{\pm}$ (single ring events)

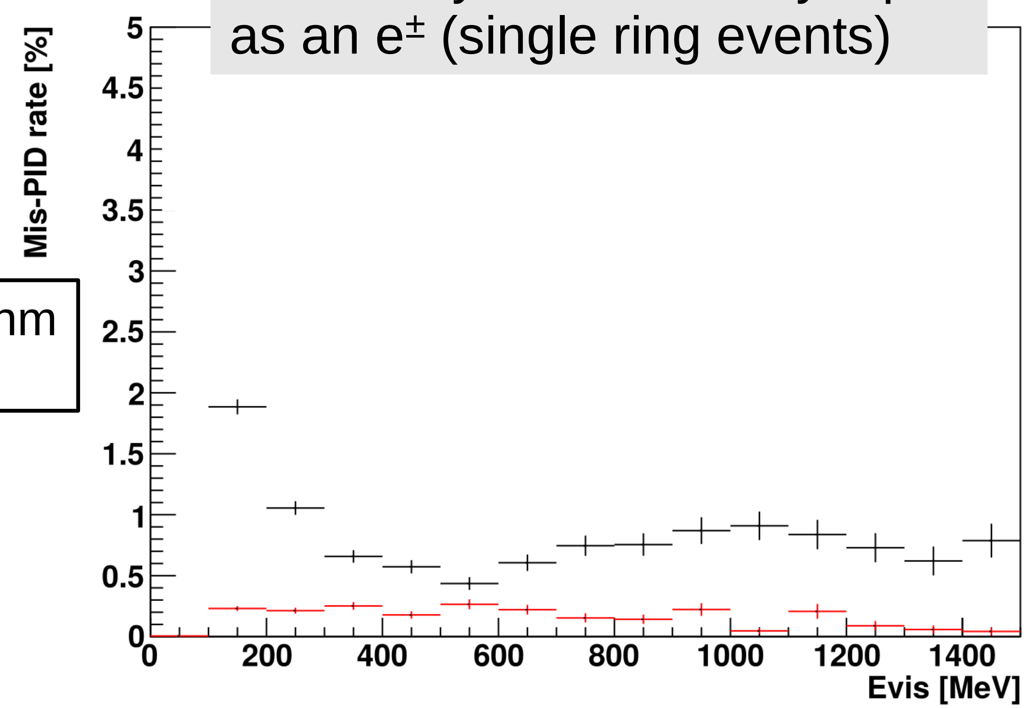

Future improvements
Neutron tagging

- Neutrons cannot be directly seen in Super-K
- Can be detected from gammas emitted during their capture
- **SK-IV**: can use capture on hydrogen **efficiency~20%** (paper in preparation)

SK preliminary

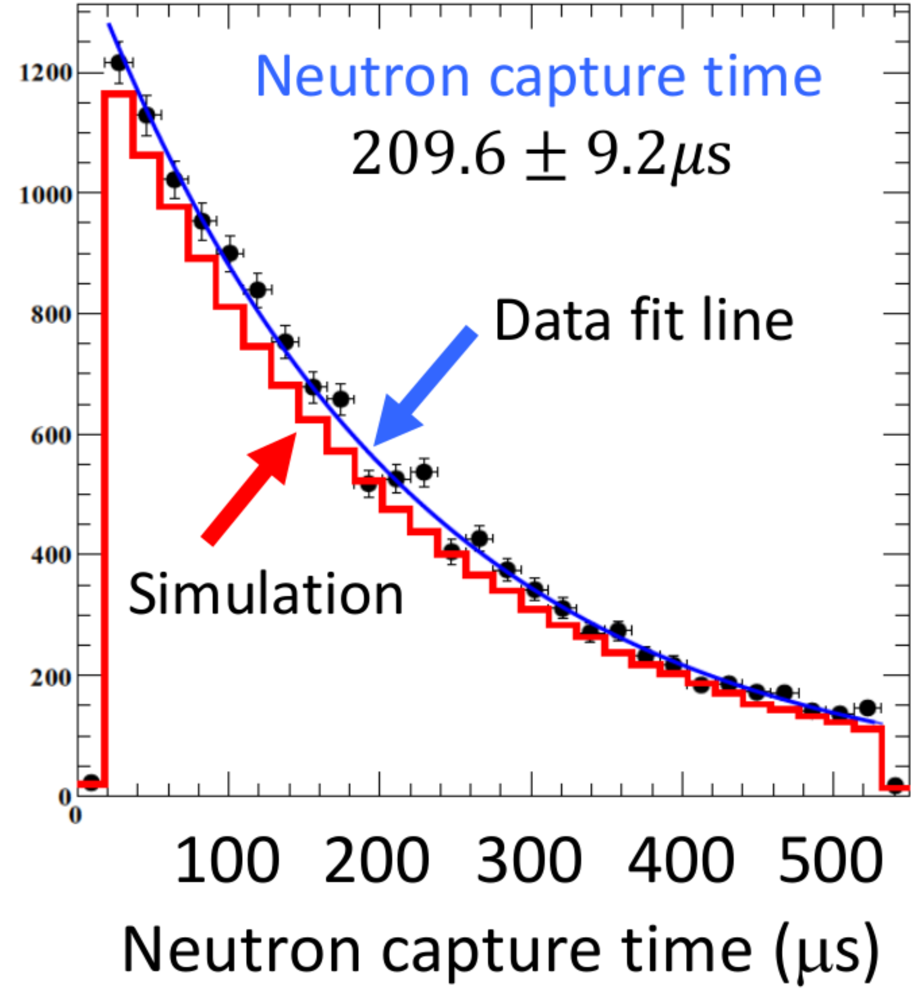

<u>Possible benefits:</u>

- ✓ statistical $\nu_e/\bar{\nu}_e$ separation in Sub-GeV samples for δ
- ✓ Improve statistical $\nu_e/\bar{\nu}_e$ separation in Multi-GeV samples for MH
- ✓ Correct for missing (invisible) energy to improve energy resolution

Detection method established, but challenges for analysis: prediction and systematic uncertainties on multiplicities

Future improvements
Neutron tagging with Gd

- Gd: large neutron capture cross-section
- Signal is easier to detect than for H capture
- Future **SK-Gd**: use capture on Gd by dissolving Gd in SK water
- **Efficiency~80%** at 0.1% Gd loading

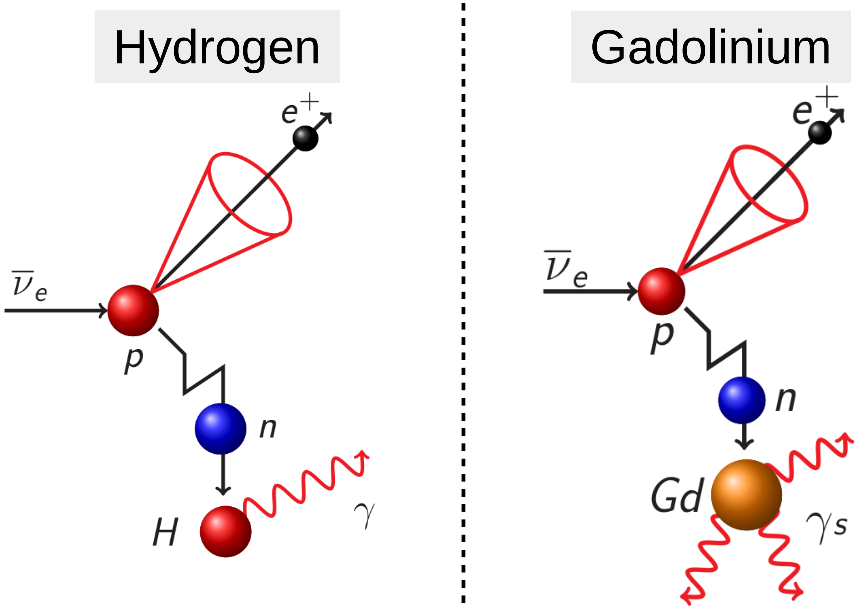

Single 2.2 MeV γ

8 MeV γ cascade

SK tank currently being refurbished to prepare for SK-Gd

Summary

- Super-K is sensitive to the mass hierarchy through a matter induced resonance in the muon to electron flavor oscillation probability and to the value of δ_{CP} through the Sub-GeV electron like events

- The T2K data can be used to constrain the values of the oscillation parameters, particularly $\sin^2(\theta_{23})$, to increase MH sensitivity

- Using 328 kton-years of atmospheric data, the NH is favored by between 81.9% and 96.7% depending on true values of oscillation parameters, and between 91.9% and 94.5% with the addition of the T2K data

- Performed search for ν_τ events appearing from oscillations.

  No ν_τ appearance hypothesis excluded at 4.6

  Measured flux averaged cross section of $(0.94 \pm 0.20) \times 10^{-38}$ cm^2, consistent with MC predictions within 1.5σ

Additional slides

Neutrino oscillations

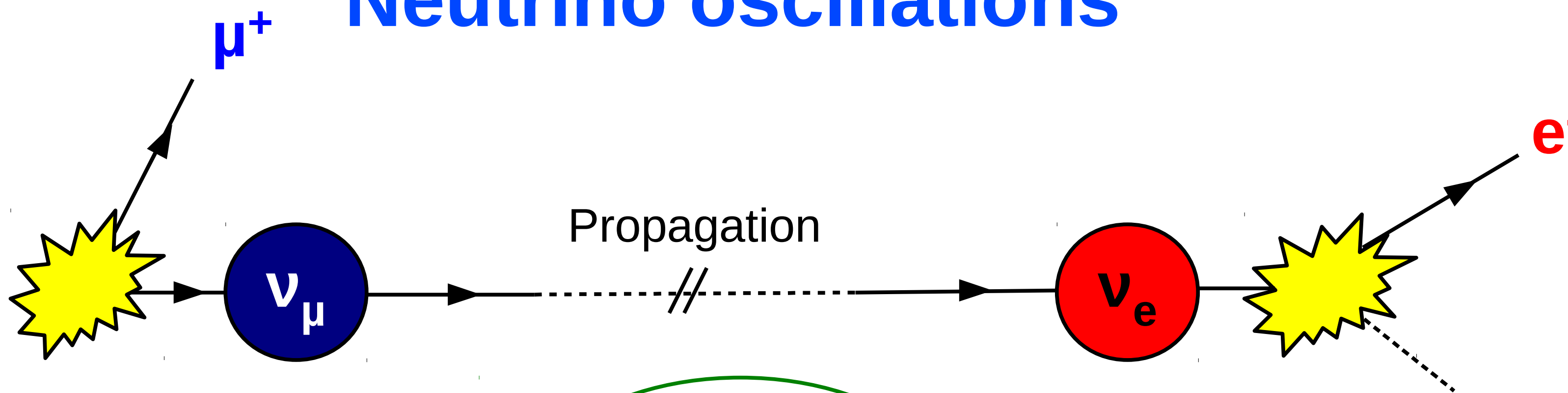

Flavor eigenstates (interaction)

$$\begin{pmatrix}\nu_e\\ \nu_\mu\\ \nu_\tau\end{pmatrix} = \begin{pmatrix}U_{e1} & U_{e2} & U_{e3}\\ U_{\mu 1} & U_{\mu 2} & U_{\mu 3}\\ U_{\tau 1} & U_{\tau 2} & U_{\tau 3}\end{pmatrix} \times \begin{pmatrix}\nu_1\\ \nu_2\\ \nu_3\end{pmatrix}$$

Mass eigenstates (propagation)

Mixing (or Pontecorvo-Maki-Nagawa-Sakata) matrix
link between the two sets of eigenstates

$P(\nu_\alpha \to \nu_\beta)$ oscillates as a function of distance L traveled by the neutrino

- Amplitude of oscillations depends on the mixing matrix U
- Phase of the oscillation depends on energy and difference of mass squared: $\mathbf{\Delta m^2_{ij} L/E}$

$(\Delta m^2_{ij} = m^2_i - m^2_j)$

Neutrino oscillations Parameters

In practice, for neutrino oscillations:

$$U = \begin{pmatrix} 1 & 0 & 0 \\ 0 & c_{23} & s_{23} \\ 0 & -s_{23} & c_{23} \end{pmatrix} \begin{pmatrix} c_{13} & 0 & s_{13}e^{-i\delta} \\ 0 & 1 & 0 \\ -s_{13}e^{i\delta} & 0 & c_{13} \end{pmatrix} \begin{pmatrix} c_{12} & s_{12} & 0 \\ -s_{12} & c_{12} & 0 \\ 0 & 0 & 1 \end{pmatrix}$$

"Atmospheric" "Reactor" "Solar"

($c_{ij} = \cos(\theta_{ij})$, $s_{ij} = \sin(\theta_{ij})$)

$P(\nu_\alpha \rightarrow \nu_\beta)$ depends on **6 parameters**:

- 3 mixing angles $\boldsymbol{\theta_{12}, \theta_{23}, \theta_{13}}$
- 2 independent mass splittings $\boldsymbol{\Delta m^2_{ij}}$
- 1 complex phase, the CP phase $\boldsymbol{\delta}$

- Observed both disappearance and appearance of neutrino flavors
- All mass splittings (Δm^2_{ij}) and mixing angles (θ_{ij}) measured to be non-zero
- Only δ still unknown (not well constrained by data)
- Sign of $\Delta m^2_{32/31}$ unknown

Atmospheric neutrino oscillations
Matter effects

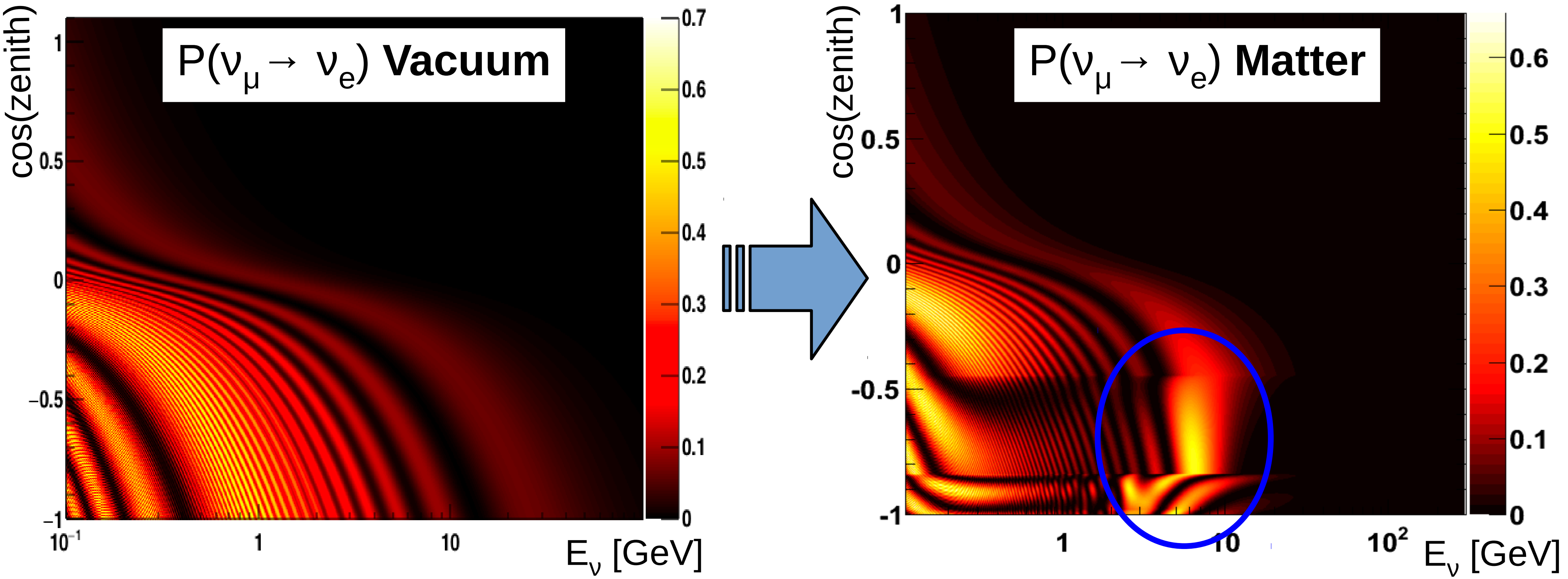

Presence of a resonance driven by θ_{13} induced matter effects between 2 and 10 GeV

- Only for ν in NH and $\bar{\nu}$ in IH → sensitivity to the mass hierarchy
- Size of the effect depends on $\sin^2(\theta_{23})$ → sensitive to θ_{23} octant
- MH sensitivity increases with larger statistics, improved ability to separate interactions of ν and $\bar{\nu}$ and constraint on $\sin^2(\theta_{23})$

Atmospheric neutrino oscillations
Matter effects – muon neutrinos

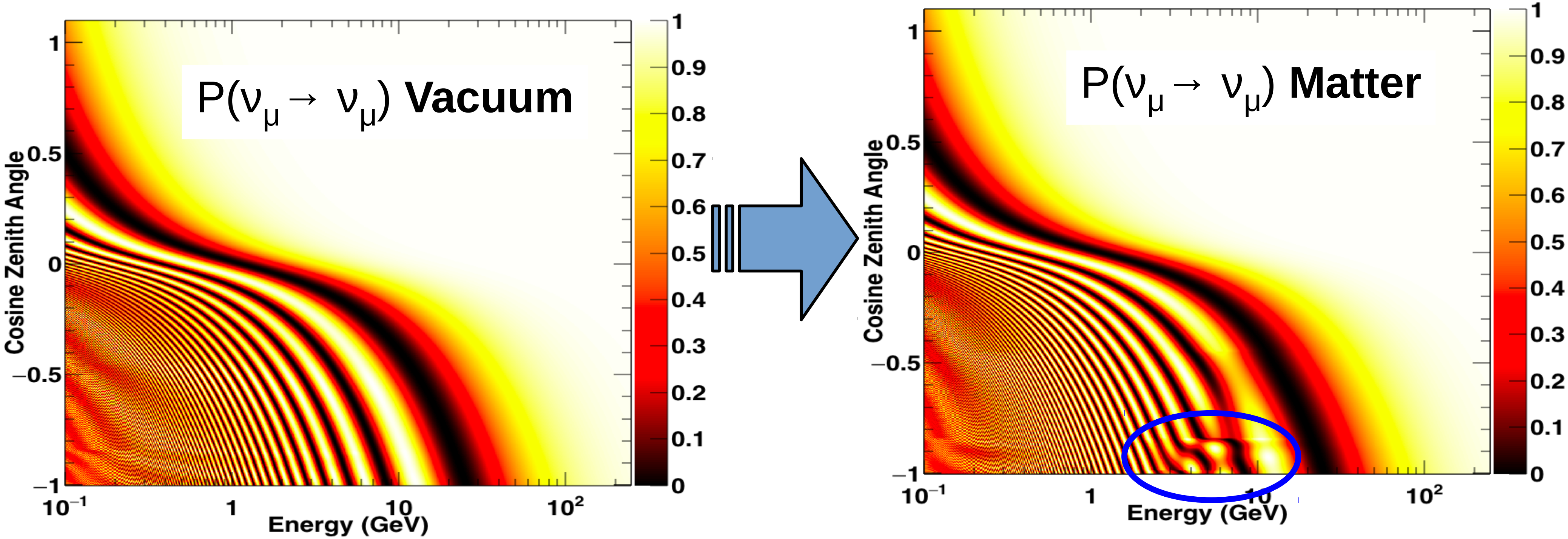

Slightly more muon disappearance for neutrinos passing through the Earth’s core

Atmospheric neutrino oscillations
Delta CP

Value of δ_{CP} modifies the oscillation patterns in a complicated way

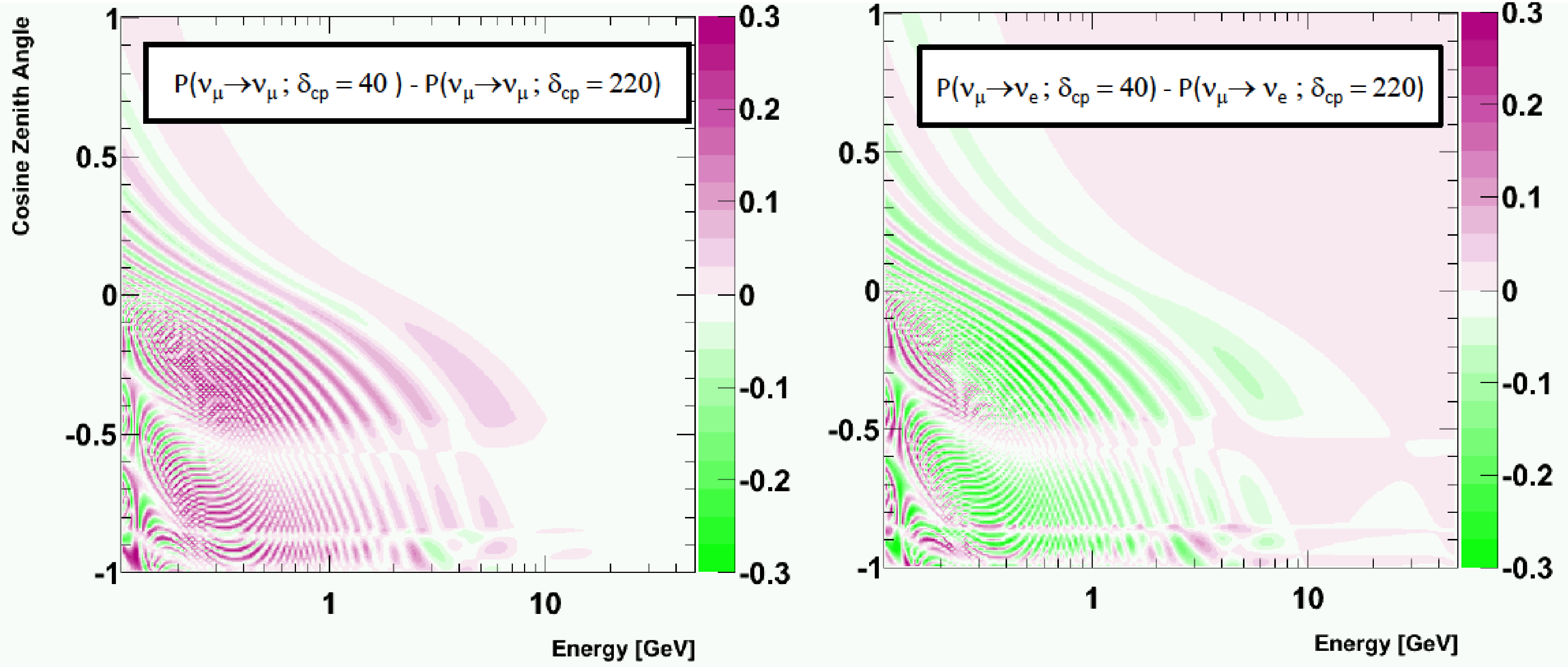

- Given neutrino flux and detector energy and angular resolution, sensitivity mainly comes from number of sub-GeV e-like events
- More ν_e appearance events for δ~220-240º, and less for δ~40-45º

Analysis strategy
Binning

Bin events in variables related to neutrino energy and propagation length: **visible** energy and **lepton** direction (1 ring) or generalized momentum direction (multi-ring)

Flux is approximatively up/down symmetric at high energy:

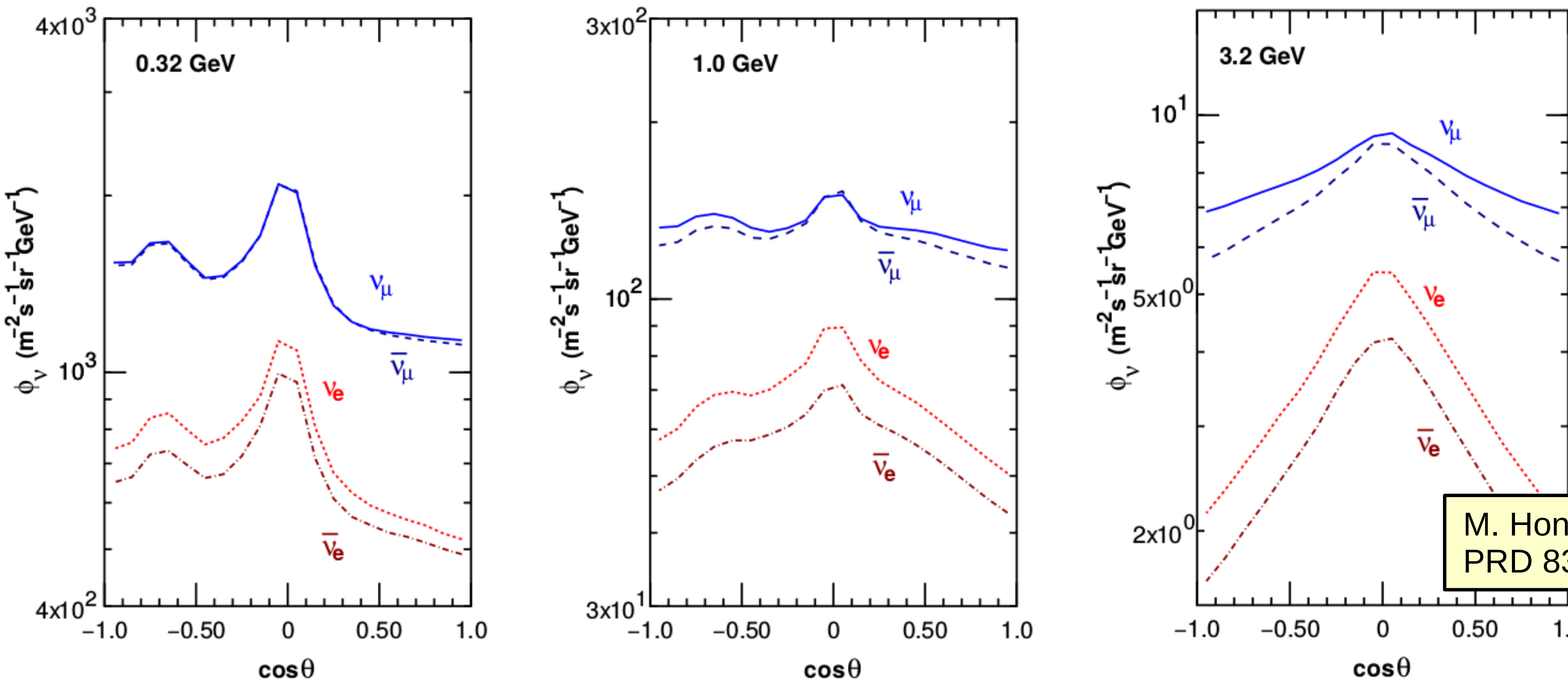

M. Honda et al.
PRD 83 (2011)

High energy down going neutrinos did not oscillate
→ systematic cancellation for this region by using up/down symmetric binning

Analysis strategy
Samples

CC ν_τ interactions disfavored at SK energies: mostly studying $P(\nu_\mu \rightarrow \nu_\mu)$, $P(\nu_e \rightarrow \nu_e)$, $P(\nu_\mu \leftrightarrow \nu_e)$ and corresponding oscillations for $\bar{\nu}$
→ **separate events between e-like and μ-like** based on PID of most energetic ring

Make **samples enriched in events of different neutrino energy regions, and interaction types** based on topology of the events, number of rings, Michel electrons and amount of visible energy

CCQE

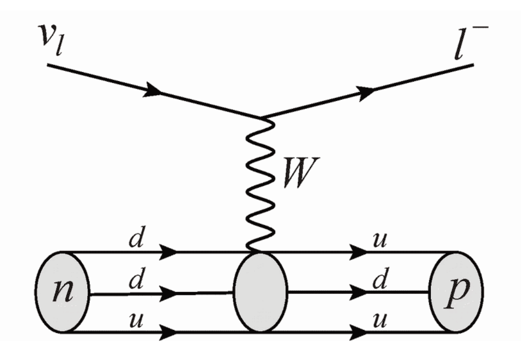

CC RES

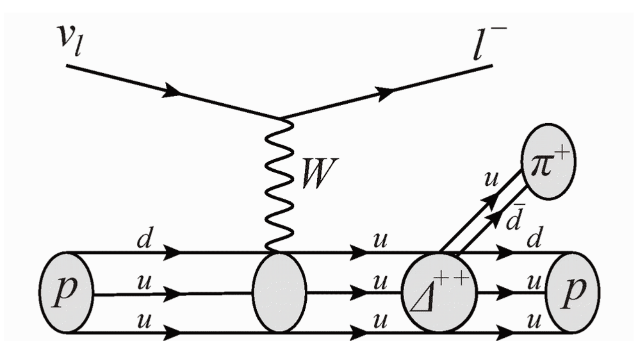

CC DIS/Multi-pi

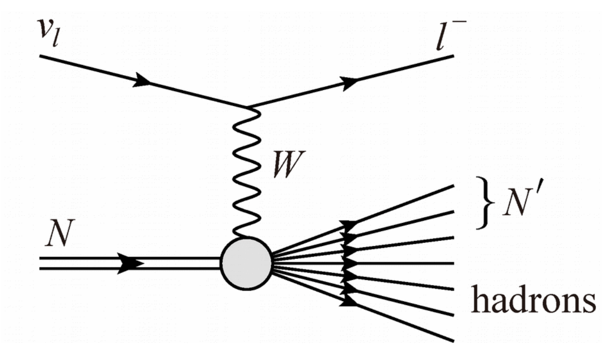

Additional **statistical separation between ν_e-like and $\bar{\nu}_e$-like for Multi-GeV e-like events** to increase sensitivity to the mass hierarchy

Monte Carlo simulation

Analysis based full MC simulation of neutrino interactions in the detector. Total MC statistics corresponds to 2000 years of atmospheric neutrino interactions

Flux: **Honda 2011**
(PRD 83, 123001 (2011))

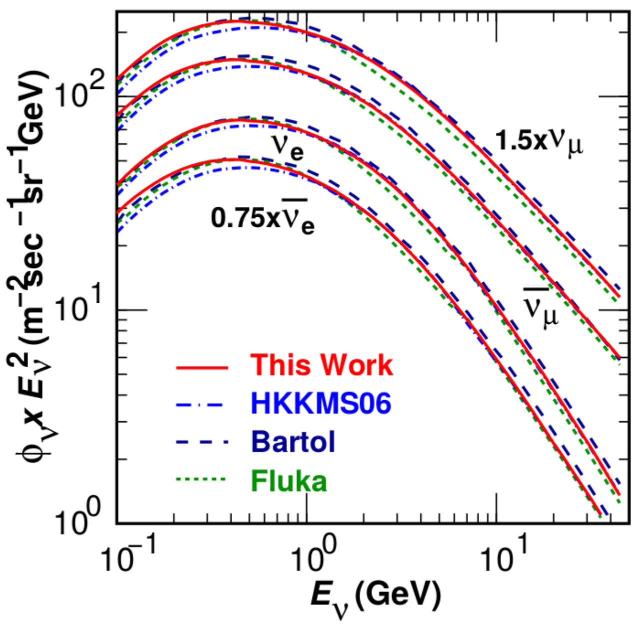

Neutrino interactions: **NEUT 5.3.6**

- CCQE: Llewellyn-Smith formalism with Smith-Moniz RFG and BBA05 form factors
- 2p2h: model from Nieves et al.
- Resonant pion production: Rein-Sehgal model with form factors from Graczyk and Sobczyk
- DIS: quark parton model using GRV98 PDFs with low q2 corrections by Bodek and Yang. PYTHIA 5.72 for high W part, custom model below
- Specific model for ν_τ interactions

Detector simulation: SKDetsim

- Based on GEANT3 (Fortran)
- NEUT cascade model used for re-interaction of pions in water (“secondary interactions”)

Event selection Topology

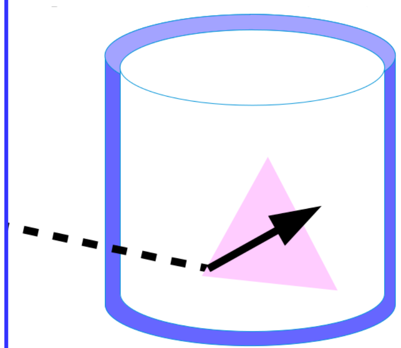

- Interaction in FV, no OD activity
- Sub-GeV (Evis<1.33 GeV) and MultiGeV
- $<E_\nu>$ ~ 1 GeV
- 8.3 evts/day

FC

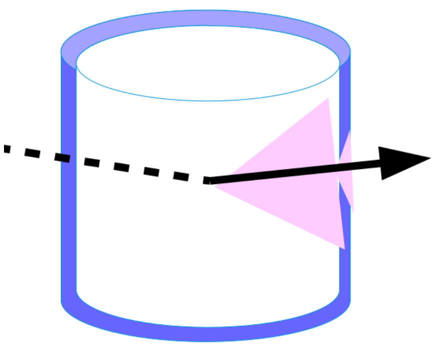

- Interaction in FV + OD activity
- Stopping and through going
- $<E_\nu>$ ~ 10 GeV
- 0.73 evts/day

PC

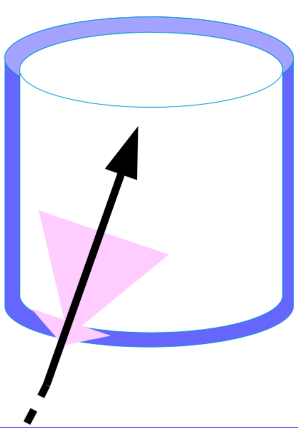

- Interaction in rock or OD
- Through going (showering and non-showering) and stopping
- $<E_\nu>$ ~ 100 GeV
- 1.49 evts/day

Upmu

Resonance region

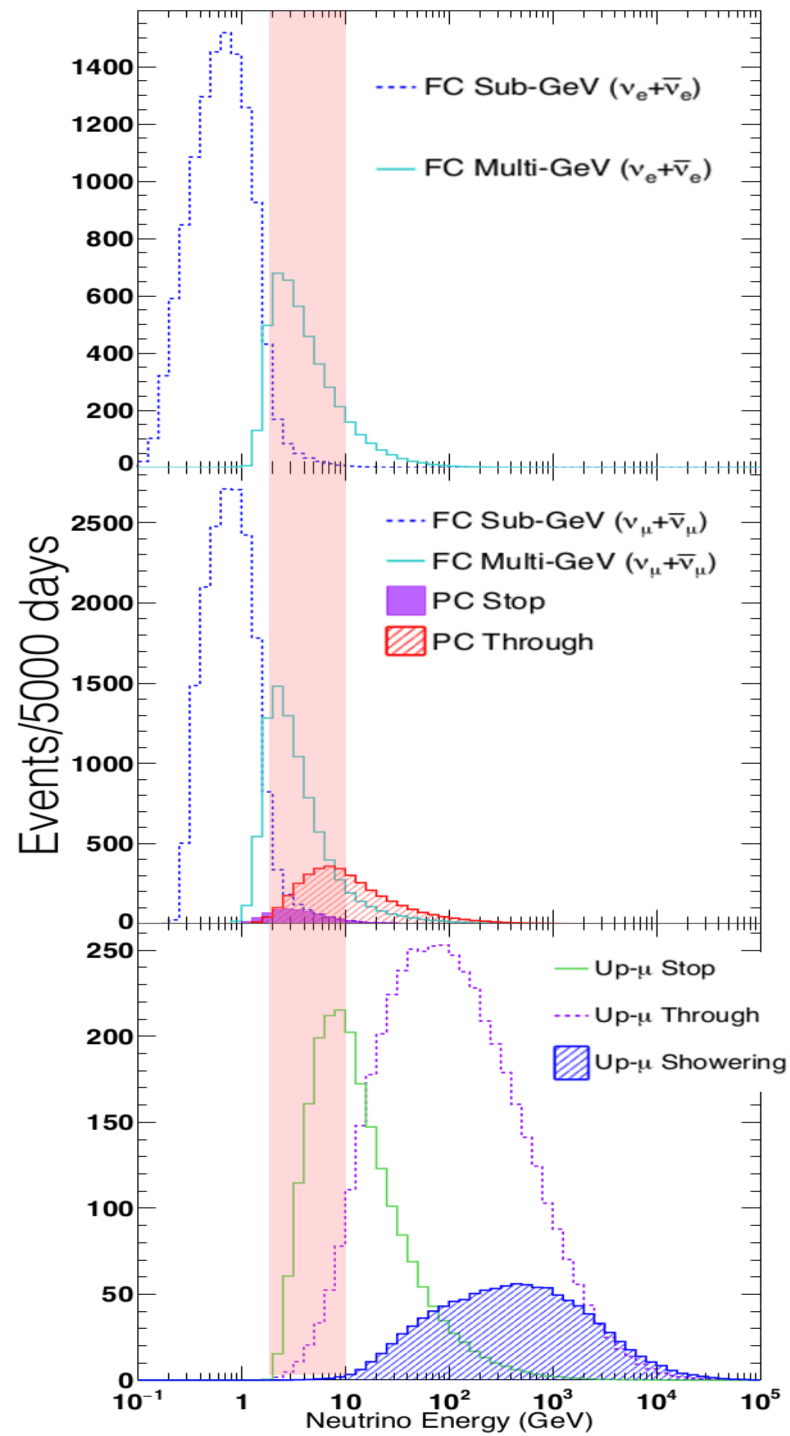

Event selection
FC Multi-GeV events

Additional selections for Fully Contained Multi-GeV (E_{vis}>1.33 GeV) to make samples enriched in ν_e and $\bar{\nu}_e$ events to increase MH sensitivity

Single ring

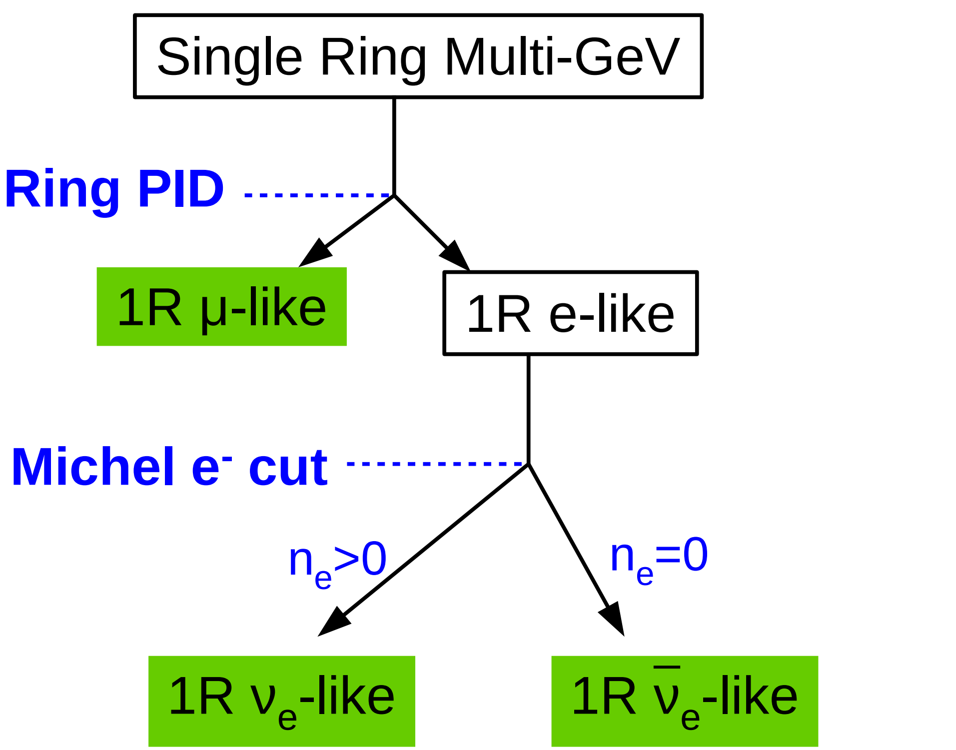

π^- from CC1π interaction of $\bar{\nu}_e$ easily captured by O^{16}
→ less likely to have a Michel electron

Multi-ring

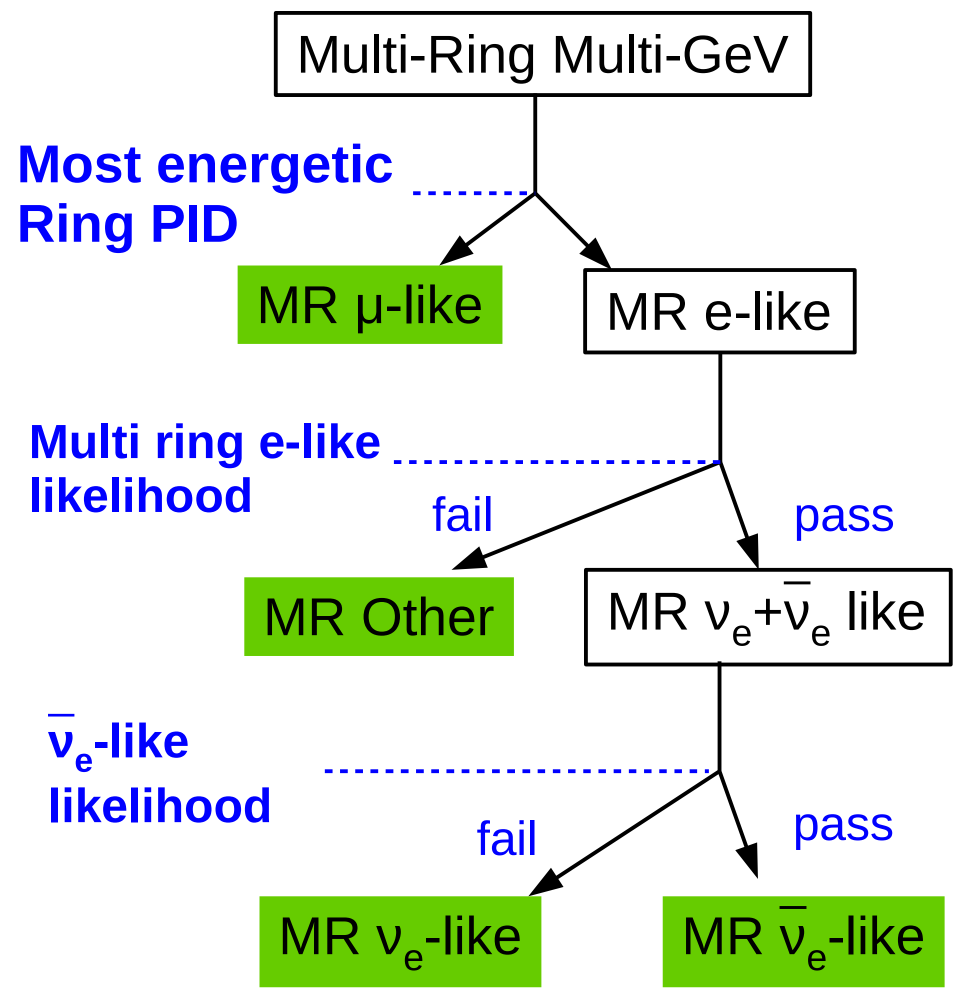

Event selection
FVFC multi-ring multi-GeV events - 1

First likelihood aims at removing NC and $\nu_\mu/\bar{\nu}_\mu$ events which ended up in the MR e-like sample due to reduced PID performance for multi-ring events

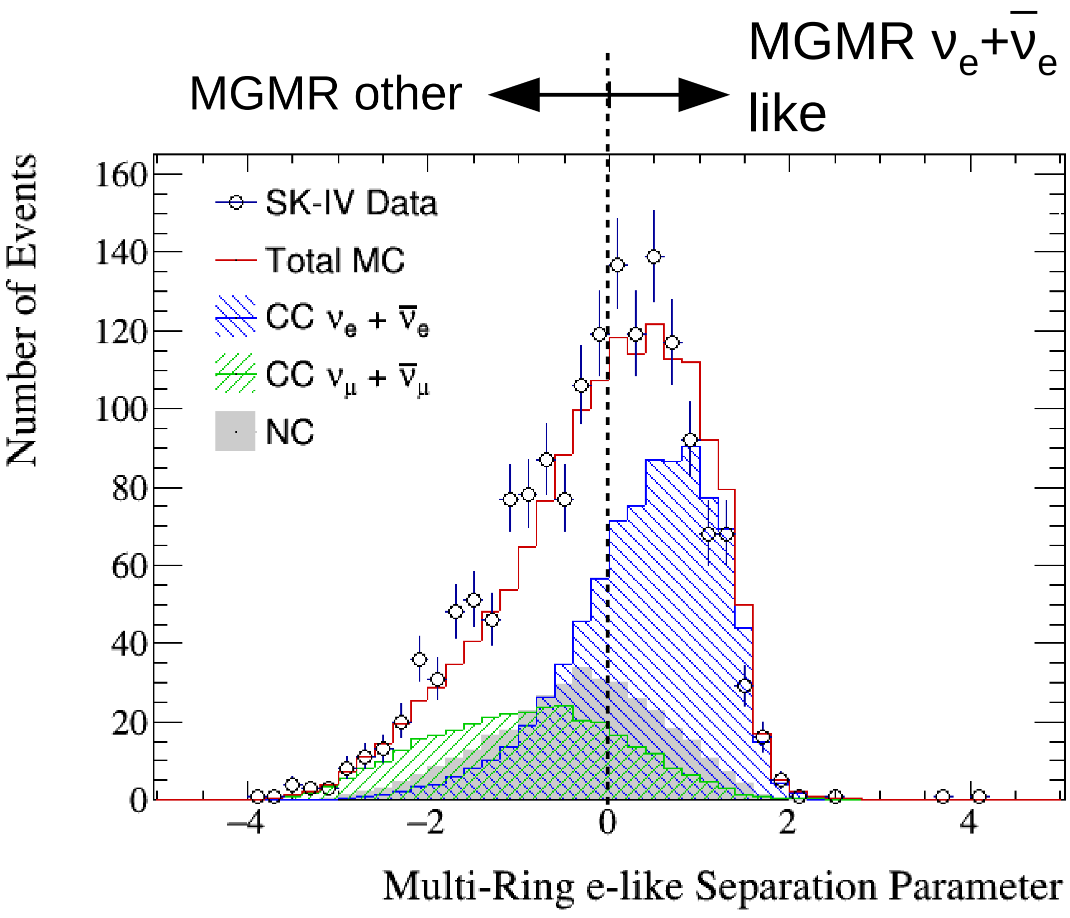

4 variables:

- PID of most energetic ring
- Momentum fraction of m.e.r
- Nb of Michel electrons
- Largest distance between a Michel electron vertex and primary vertex

Signal: CC ν_e and $\bar{\nu}_e$ interactions
Efficiency (signal): 72.7%
Purity: 73%

Event selection
FVFC multi-ring multi-GeV events - 2

Second likelihood is the real statistical separation between ν_e and $\bar{\nu}_e$ events

Dominant interaction is CC DIS

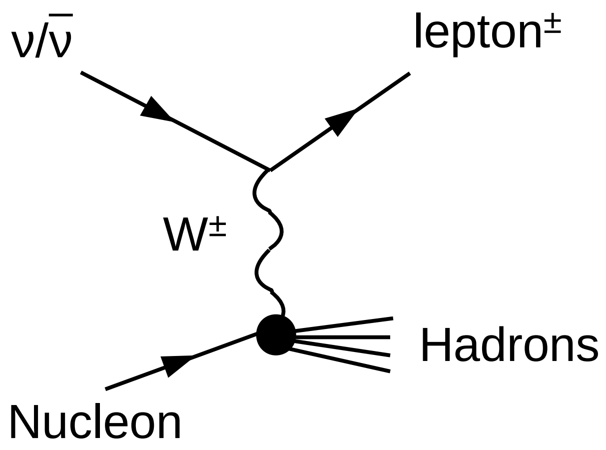

Larger transferred energy fraction (Bjorken y) for ν than $\bar{\nu}$

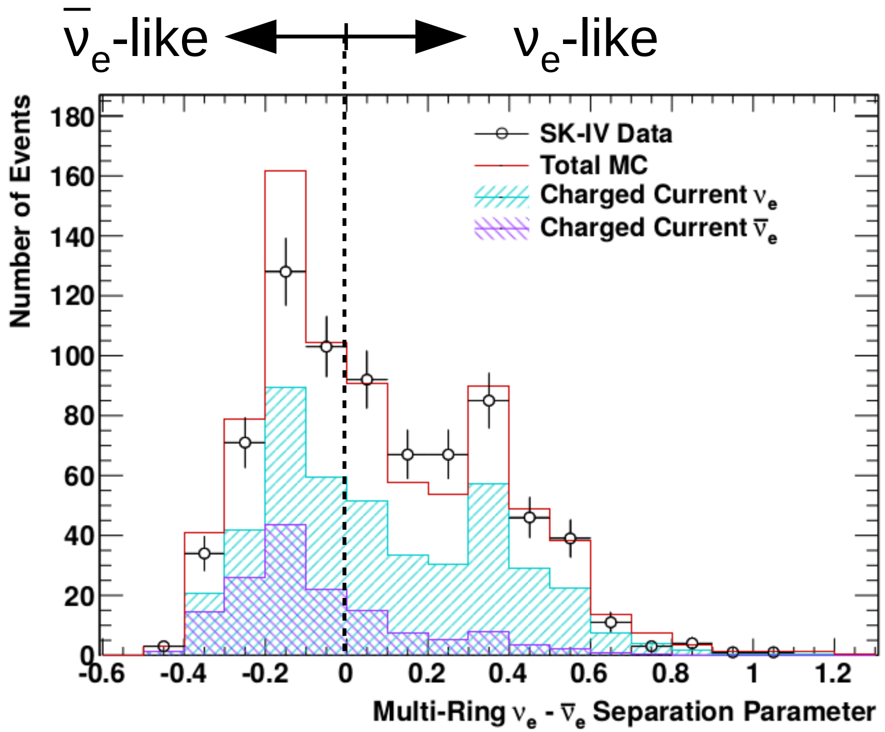

	Neutrino	Anti-neutrino
Nb of rings	More	Less
Nb of Michel e-	More	Less
Transverse momentum	Larger	smaller

	Efficiency (signal)	Purity
ν_e-like	52.9%	58.4%
$\bar{\nu}_e$-like	71%	27.5%

Atmospheric neutrino results
Contributions to the MH preference

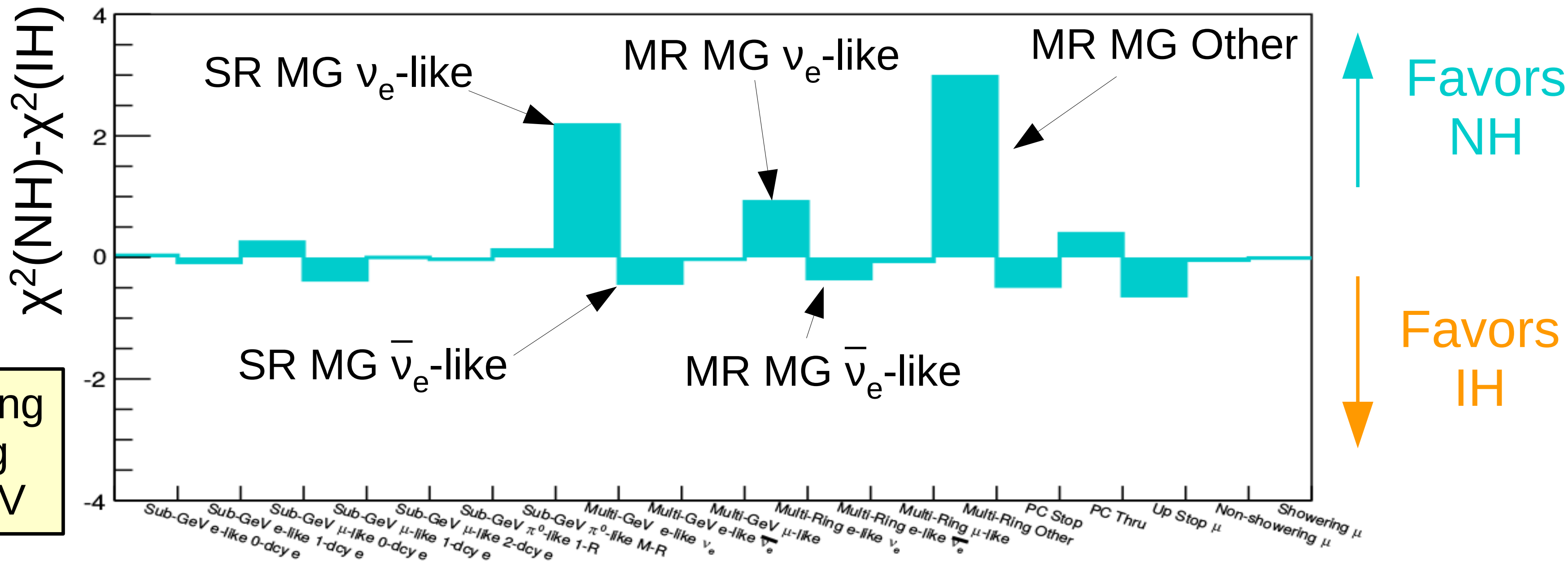

SR: Single Ring
MR: Multi-ring
MG: Multi-GeV

- Contribution to $\Delta\chi^2$ comes mainly from Multi-GeV e-like samples
- MR Other sample has the biggest contribution, although it has lower purity
- Large statistical errors: statistically limited

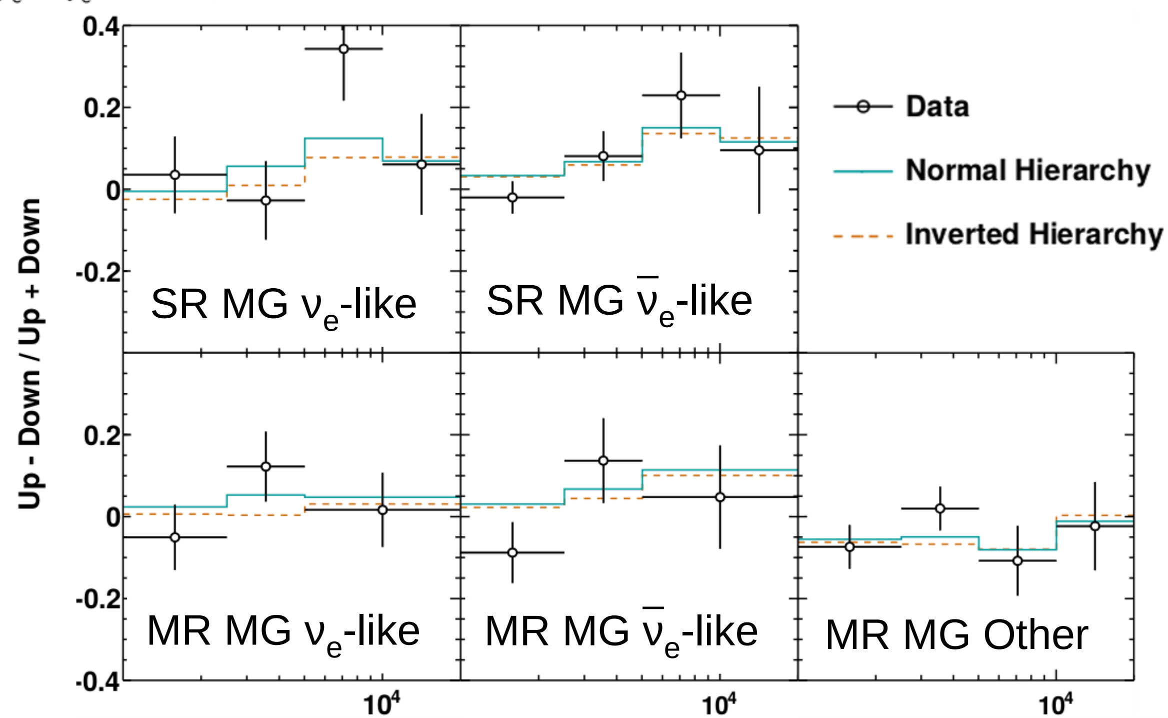

Atmospheric neutrino results
Search for matter effects

- Test consistency of data with matter effect
- Use all changes compared to vacuum oscillations, not just hierarchy dependent ones
- Introduce multiplicative parameter α which changes electron density
- Best fit for α=1 and NH
- Disfavors vacuum oscillation at $\Delta\chi^2$=5.2 (1.6σ)

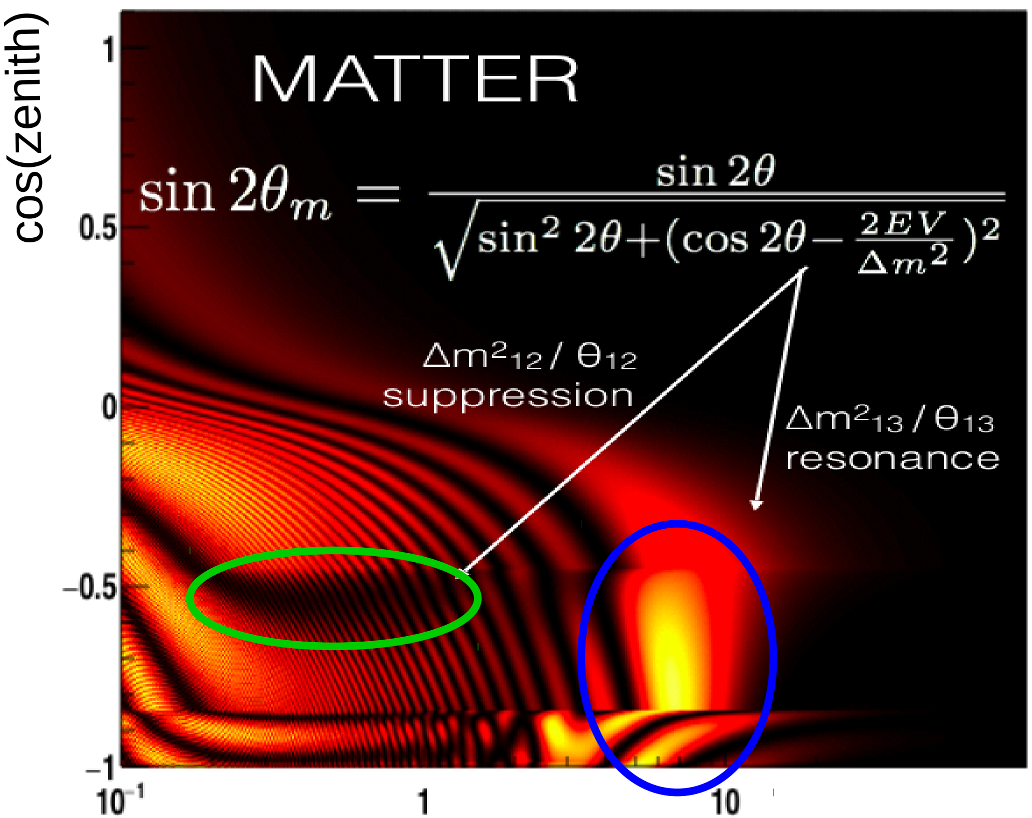

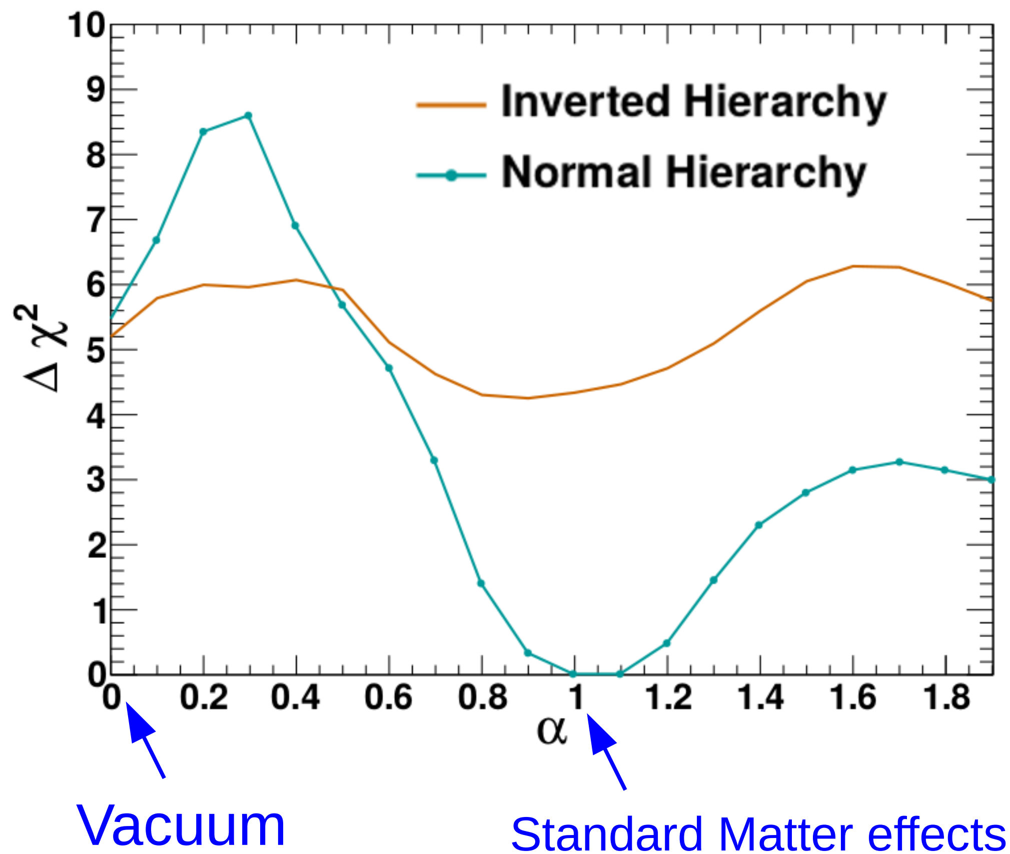

MC predictions

Sample	Energy bins	$\cos\theta_z$ bins	CC ν_e	CC $\bar{\nu}_e$	CC $\nu_\mu + \bar{\nu}_\mu$	CC ν_τ	NC	Data	MC
Fully Contained (FC) Sub-GeV									
e-like, Single-ring									
0 decay-e	5 $e^\pm$ momentum	10 in $[-1, 1]$	0.717	0.248	0.002	0.000	0.033	10294	10266.1
1 decay-e	5 $e^\pm$ momentum	single bin	0.805	0.019	0.108	0.001	0.067	1174	1150.7
μ-like, Single-ring									
0 decay-e	5 $\mu^\pm$ momentum	10 in $[-1, 1]$	0.041	0.013	0.759	0.001	0.186	2843	2824.3
1 decay-e	5 $\mu^\pm$ momentum	10 in $[-1, 1]$	0.001	0.000	0.972	0.000	0.027	8011	8008.7
2 decay-e	5 $\mu^\pm$ momentum	single bin	0.000	0.000	0.979	0.001	0.020	687	687.0
π^0-like									
Single-ring	5 $e^\pm$ momentum	single bin	0.096	0.033	0.015	0.000	0.856	578	571.8
Two-ring	5 π^0 momentum	single bin	0.067	0.025	0.011	0.000	0.897	1720	1728.4
Multi-ring			0.294	0.047	0.342	0.000	0.318	(1682)	(1624.2)
Fully Contained (FC) Multi-GeV									
Single-ring									
ν_e-like	4 $e^\pm$ momentum	10 in $[-1, 1]$	0.621	0.090	0.100	0.033	0.156	705	671.3
$\bar{\nu}_e$ -like	4 $e^\pm$ momentum	10 in $[-1, 1]$	0.546	0.372	0.009	0.010	0.063	2142	2193.7
μ-like	2 $\mu^\pm$ momentum	10 in $[-1, 1]$	0.003	0.001	0.992	0.002	0.002	2565	2573.8
Multi-ring									
ν_e -like	3 visible energy	10 in $[-1, 1]$	0.557	0.102	0.117	0.040	0.184	907	915.5
$\bar{\nu}_e$ -like	3 visible energy	10 in $[-1, 1]$	0.531	0.270	0.041	0.022	0.136	745	773.8
μ-like	4 visible energy	10 in $[-1, 1]$	0.027	0.004	0.913	0.005	0.051	2310	2294.0
Other	4 visible energy	10 in $[-1, 1]$	0.275	0.029	0.348	0.049	0.299	1808	1772.6
Partially Contained (PC)									
Stopping	2 visible energy	10 in $[-1, 1]$	0.084	0.032	0.829	0.010	0.045	566	570.0
Through-going	4 visible energy	10 in $[-1, 1]$	0.006	0.003	0.978	0.007	0.006	2801	2889.9
Upward-going Muons (Up-μ)									
Stopping	3 visible energy	10 in $[-1, 0]$	0.008	0.003	0.986	0.000	0.003	1456.4	1448.9
Through-going									
Non-showering	single bin	10 in $[-1, 0]$	0.002	0.001	0.996	0.000	0.001	5035.3	4900.4
Showering	single bin	10 in $[-1, 0]$	0.001	0.000	0.998	0.000	0.001	1231.0	1305.0

328 kton-year, $\sin^2(\theta_{23})$=0.5, Δm^2_{32}=2.4e-3

Atmospheric neutrino results
Data/MC comparisons

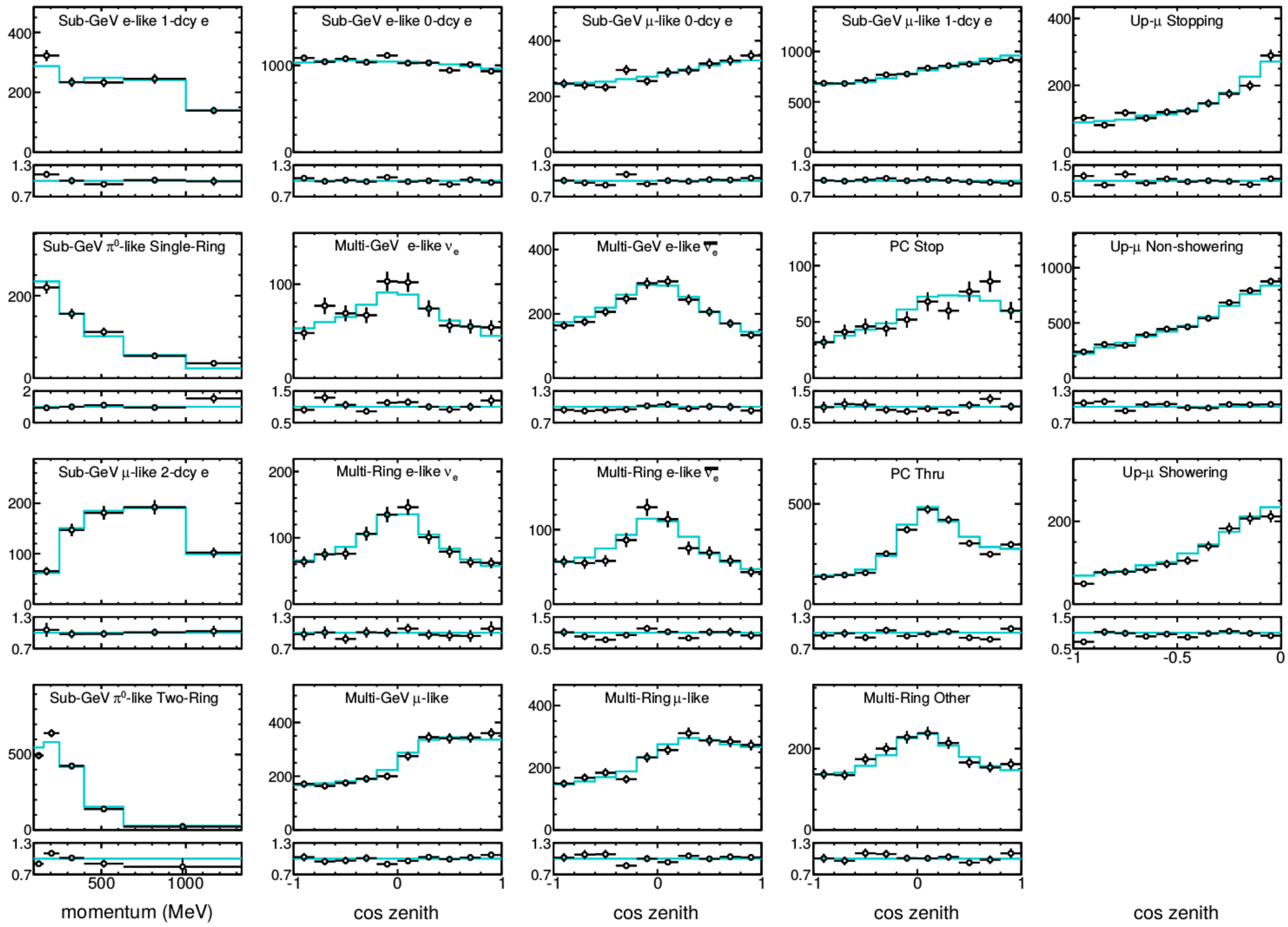

Flux systematics

Systematic error			Fit value (%)	σ (%)
Flux normalization	$E_\nu < 1$ GeV[a]		14.3	25
	$E_\nu > 1$ GeV[b]		7.8	15
$(\nu_\mu + \bar{\nu}_\mu)/(\nu_e + \bar{\nu}_e)$	$E_\nu < 1$ GeV		0.08	2
	$1 < E_\nu < 10$ GeV		−1.1	3
	$E_\nu > 10$ GeV[c]		1.6	5
$\bar{\nu}_e/\nu_e$	$E_\nu < 1$ GeV		1.6	5
	$1 < E_\nu < 10$ GeV		3.3	5
	$E_\nu > 10$ GeV[d]		−1.6	8
$\bar{\nu}_\mu/\nu_\mu$	$E_\nu < 1$ GeV		0.24	2
	$1 < E_\nu < 10$ GeV		2.9	6
	$E_\nu > 10$ GeV[e]		−2.9	15
Up/down ratio	<400 MeV	e-like	−0.026	0.1
		μ-like	−0.078	0.3
		0-decay μ-like	−0.286	1.1
	>400 MeV	e-like	−0.208	0.8
		μ-like	−0.130	0.5
		0-decay μ-like	−0.442	1.7
	Multi-GeV	e-like	−0.182	0.7
		μ-like	−0.052	0.2
	Multi-ring Sub-GeV	e-like	−0.104	0.4
		μ-like	−0.052	0.2
	Multi-ring Multi-GeV	e-like	−0.078	0.3
		μ-like	−0.052	0.2
	PC		−0.052	0.2
Horizontal/vertical ratio	<400 MeV	e-like	0.018	0.1
		μ-like	0.018	0.1
		0-decay μ-like	0.054	0.3
	>400 MeV	e-like	0.252	1.4
		μ-like	0.341	1.9
		0-decay μ-like	0.252	1.4
	Multi-GeV	e-like	0.576	3.2
		μ-like	0.414	2.3
	Multi-ring Sub-GeV	e-like	0.252	1.4
		μ-like	0.234	1.3
	Multi-ring Multi-GeV	e-like	0.504	2.8
		μ-like	0.270	1.5
	PC		0.306	1.7
K/π ratio in flux calculation[f]			−9.3	10
Neutrino path length			−2.13	10
Sample-by-sample	FC Multi-GeV		−6.6	5
	PC + Stopping UP-μ		0.22	5
Matter effects			0.52	6.8

Interaction and oscillation systematics

Systematic error		Fit value (%)	σ (%)
M_A in QE		−0.69	10
Single π Production, Axial Coupling		−4.4	10
Single π Production, C_{A5}		−3.1	10
Single π Production, BKG		−8.7	10
CCQE cross section[a]		6.7	10
CCQE $\bar{\nu}/\nu$ ratio[a]		9.2	10
CCQE μ/e ratio[a]		0.67	10
DIS cross section		−4.4	5
DIS model comparisons[b]		3.0	10
DIS Q^2 distribution (high W)[c]		8.2	10
DIS Q^2 distribution (low W)[c]		−5.8	10
Coherent π production		−10.0	100
NC/CC		12.1	20
ν_τ cross section		−13.8	25
Single π production, $\pi^0/\pi^\pm$		−20.3	40
Single π production, $\bar{\nu}_i/\nu_i$ (i = e, μ)[d]		−11.0	10
NC fraction from hadron simulation		−0.47	10
π^+ decay uncertainty Sub-GeV 1-ring	e-like 0-decay	−0.17	0.6
	μ-like 0-decay	−0.22	0.8
	e-like 1-decay	1.1	4.1
	μ-like 1-decay	0.25	0.9
	μ-like 2-decay	1.60	5.7
Final state and secondary interactions[e]		−0.2	10
Meson exchange current[f]		−1.8	10
$\Delta m^2{}_{21}$ [29]		0.022	2.4
$\sin^2(\theta_{12})$ [29]		0.32	4.6
$\sin^2(\theta_{13})$ [29]		0.11	5.4

Reduction and background systematics

Systematic Error		SK-I Fit Value	SK-I σ	SK-II Fit Value	SK-II σ	SK-III Fit Value	SK-III σ	SK-IV Fit Value	SK-IV σ
FC reduction		−0.009	0.2	0.005	0.2	0.066	0.8	0.68	1.3
PC reduction		0.016	2.4	−3.43	4.8	−0.012	0.5	−0.78	1
FC/PC separation		−0.10	0.6	0.077	0.5	−0.13	0.9	0.0004	0.02
PC stopping/through-going separation (bottom)		−15.8	23	−2.4	13	−0.32	12	−1.5	6.8
PC stopping/through-going separation (barrel)		3.8	7	−5.7	9.4	−13.9	29	−0.40	8.5
PC stopping/through-going separation (top)		8.5	46	−3.0	19	−12.6	87	−24.1	40
Non-ν background	Sub-GeV μ-like	0.010	0.1	0.065	0.4	0.105	0.5	−0.011	0.02
	Multi-GeV μ-like	0.040	0.4	0.065	0.4	0.105	0.5	−0.011	0.02
	Sub-GeV 1-ring 0-decay μ-like	0.010	0.1	0.049	0.3	0.084	0.4	−0.052	0.09
	PC	0.020	0.2	0.115	0.7	0.381	1.8	−0.282	0.49

(Table continued)

Systematic Error			SK-I Fit Value	SK-I σ	SK-II Fit Value	SK-II σ	SK-III Fit Value	SK-III σ	SK-IV Fit Value	SK-IV σ
	Sub-GeV e-like (flasher event)		0.068	0.5	0.000	0.2	−0.004	0.2	−0.000	0.02
	Multi-GeV e-like (flasher event)		0.014	0.1	0.000	0.3	−0.014	0.7	−0.000	0.08
	Multi-GeV 1-ring e-like		3.6	13	−5.2	38	−1.0	27	2.6	18
	Multi-GeV Multi-ring e-like		3.7	12	3.8	11	0.75	11	0.34	12
Fiducial Volume			−0.85	2	−0.11	2	0.22	2	−1.5	2
Ring separation	<400 MeV	e-like	0.45	2.3	−1.07	1.3	0.80	2.3	0.96	1.6
		μ-like	0.14	0.7	−1.91	2.3	1.04	3	1.79	3
	>400 MeV	e-like	0.078	0.4	−1.40	1.7	0.45	1.3	−0.60	1
		μ-like	0.14	0.7	−0.576	0.7	0.208	0.6	−0.36	0.6
	Multi-GeV	e-like	0.72	3.7	−2.14	2.6	0.45	1.3	−0.60	1
		μ-like	0.33	1.7	−1.41	1.7	0.35	1	0.72	1.2
	Multi-ring Sub-GeV	e-like	−0.68	3.5	3.13	3.8	0.45	1.3	1.14	1.9
		μ-like	−0.88	4.5	6.75	8.2	−0.90	2.6	1.37	2.3
	Multi-ring Multi-GeV	e-like	−0.61	3.1	1.56	1.9	−0.38	1.1	0.54	0.9
		μ-like	−0.80	4.1	0.658	0.8	−0.73	2.1	−1.43	2.4
Particle identification (1 ring)	Sub-GeV	e-like	0.039	0.23	0.227	0.66	0.053	0.26	−0.123	0.28
		μ-like	−0.030	0.18	−0.172	0.5	−0.038	0.19	0.097	0.22
	Multi-GeV	e-like	0.032	0.19	0.082	0.24	0.062	0.31	−0.154	0.35
		μ-like	−0.032	0.19	−0.089	0.26	−0.060	0.3	0.154	0.35
Particle identification (multi-ring)	Sub-GeV	e-like	−0.23	3.1	−3.44	6	3.49	9.5	−2.24	4.2
		μ-like	0.049	0.66	1.38	2.5	−1.91	5.2	0.85	1.6
	Multi-GeV	e-like	0.48	6.5	5.57	9.7	−1.80	4.9	−1.76	3.3
		μ-like	−0.21	2.9	−2.24	3.9	0.99	2.7	0.85	1.6
Multi-ring likelihood selection	Multi-ring e-like	ν_e, $\bar{\nu}_e$	−6.5	6.0	−1.3	3.8	−5.3	5.3	−2.3	3.0
	Multi-ring Other		6.2	5.7	1.4	4.1	4.7	4.9	2.7	3.4
Energy calibration			−0.75	3.3	−0.90	2.8	0.06	2.4	0.08	2.1
Up/down asymmetry energy calibration			0.26	0.6	0.24	0.6	0.74	1.3	−0.15	0.4
UP-μ reduction	Stopping		−0.091	0.7	−0.090	0.7	0.162	0.7	0.087	0.5
	Through-going		−0.065	0.5	−0.064	0.5	0.115	0.5	0.052	0.3
UP-μ stopping/through-going separation			0.003	0.4	−0.004	0.6	0.030	0.4	−0.102	0.6
Energy cut for stopping UP-μ			−0.043	0.9	−0.122	1.3	0.957	2	−0.122	1.7
Path length cut for through-going UP-μ			−0.416	1.5	−0.826	2.3	0.993	2.8	1.47	1.5
Through-going UP-μ showering separation			7.53	3.4	−4.68	4.4	2.90	2.4	−3.30	3
Background subtraction for UP-μ	Stopping[a]		10.0	16	−3.1	21	−4.9	20	−6.7	17
	Non-showering[a]		−3.6	18	−3.6	14	1.4	24	2.1	17
	Showering[a]		−12.3	18	−15.7	14	0.1	24	−0.9	24
$\nu_e/\bar{\nu}_e$ Separation			−0.98	7.2	6.96	7.9	0.45	7.7	2.46	6.8
Sub-GeV 1-ring π^0 selection	$100 < P_e < 250$ MeV/c		1.7	9	7.0	10	0.98	6.3	5.2	4.6
	$250 < P_e < 400$ MeV/c		1.7	9.2	9.8	14	0.76	4.9	3.4	3
	$400 < P_e < 630$ MeV/c		3.0	16	7.7	11	3.7	24	14.8	13
	$630 < P_e < 1000$ MeV/c		2.6	14	11.2	16	1.3	8.2	19.4	17
	$1000 < P_e < 1330$ MeV/c		2.2	12	6.8	9.8	1.7	11	27.4	24
Sub-GeV 2-ring π^0			1.3	5.6	−2.7	4.4	1.6	5.9	−0.72	5.6
Decay-e tagging			−3.2	10	−1.0	10	0.9	10	1.3	10
Solar Activity			−1.8	20	20.0	50	2.7	20	0.6	10

Tau samples compositions and branching ratios

Interaction Mode	non-tau-like	tau-like	All
CC ν_e	3071.0	1399.2	4470.2
CC ν_μ	4231.9	783.4	5015.3
CC ν_τ	49.1	136.1	185.2
NC	291.8	548.3	840.1

TABLE I. The break down of interaction modes of both background and expected signal shown in number of events in simulation scaled to SK-I through SK-IV live time. By cutting the NN output at 0.5, each mode is separated into tau-like (NN>0.5) and non-tau-like (NN<0.5).

Decay mode	Branching ratio (%)	Tau-like fraction (%)	Branching ratio×Tau-like fraction (%)
$e^-\bar{\nu}_e\nu_\tau$	17.83	67.3±2.2	12.0±0.4
$\mu^-\bar{\nu}_\mu\nu_\tau$	17.41	42.6±2.6	7.2±0.5
$\pi^-\nu_\tau$	10.83	84.7±3.8	9.2±0.4
$\pi^-\pi^0\nu_\tau$	25.52	81.0±2.1	20.7±0.5
$3\pi\nu_\tau$	18.29	88.7±2.5	16.2±0.5
others	10.12	90.5±3.4	9.2±0.3

TABLE II. Decay modes of tau leptons with branching ratio adapted from [37], along with the fraction of tau-like events and the product of branching ratio and tau-like ratio in each mode in the Super-K simulation.